Table 3. The relationship between molecular species and mass numbers in each mycolic acid subclass

Underlining indicates a major component.

Strain		α-MA	Keto-MA	Dicarboxy-MA
KUM 060204^T	Mass number [M+Na]+	1230, 1258, 1286	1274, 1302, 1316, 1344	1024, 1038, 1052, 1066, 1080, 1094
	Molecular species (carbon-chain length)	82:2, 84:2, 86:2	84:1, 86:1, 87:1, 89:1	64:1, 65:1, 66:1, 67:1, 68:1, 69:1
NTH 512-121	Mass number [M+Na]+	1230, 1258, 1286	1302, 1316, 1344	1024, 1038, 1052, 1066, 1080, 1094
	Molecular species (carbon-chain length)	82:2, 84:2, 86:2	86:1, 87:1, 89:1	64:1, 65:1, 66:1, 67:1, 68:1, 69:1
AHM 060905	Mass number [M+Na]+	1230, 1258, 1286	1302, 1316, 1344	1024, 1038, 1052, 1066, 1080, 1094
	Molecular species (carbon-chain length)	82:2, 84:2, 86:2	86:1, 87:1, 89:1	64:1, 65:1, 66:1, 67:1, 68:1, 69:1

phylogenetic neighbours *M. celatum* ATCC 51131^T, *M. branderi* ATCC 51789^T and *M. branderi* ATCC 51788 (similarity 49.9, 44.5 and 41.5%, respectively). These results provide further evidence for the genetic diversity between this strain and closely related species, indicating that this isolate comprises a new mycobacterial species.

Based on the genotypic and phenotypic data described above, it was concluded that strain KUM 060204^T represents a novel *Mycobacterium* species for which we propose the name *Mycobacterium kyorinense* sp. nov. Two other strains, NTH 512-121 and AHM 060905, were assumed to belong to the same species as strain KUM 060204^T based on sequence identity. Considering that strains KUM 060204^T and AHM 060905 fulfil the criteria for clinical significance, this newly identified *Mycobacterium* is considered to be a potential pathogen for infection in humans.

Description of *Mycobacterium kyorinense* sp. nov.

Mycobacterium kyorinense (kyo.rin.en'se. N.L. neut. adj. *kyorinense* of Kyorin, referring to the Kyorin University Hospital where the first strain was isolated).

Long, rod-shaped cells (approx. 3 × 0.3 μm); acid–alcohol-fast. Growth requires >4 weeks at 28–42 °C. No growth occurs at 25 °C. Colony diameters are 1–2 mm on Middlebrook 7H11-OADC agar. Colonies on 1% Ogawa egg agar are smooth and raised with round or lobate regular margins, and non-chromogenic. Negative for Tween hydrolysis, nitrate reductase, semiquantitative catalase, urease activity, 3-day arylsulfatase activity, pyrazinamidase, tellurite reduction and niacin accumulation; positive for 14-day arylsulfatase activity and heat-stable catalase tests. Susceptible to clarithromycin and ethambu-

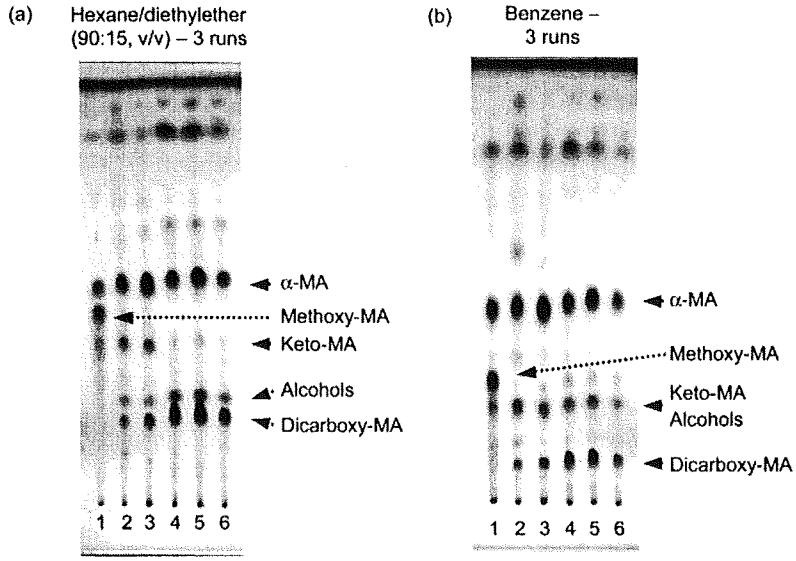

Fig. 1. TLC patterns of mycolic acid methyl esters. (a) Plate developed three times with hexane/diethylether. (b) Plate developed three times with benzene. Lanes: 1, *M. tuberculosis* H37Rv ATCC 27294^T; 2, *M. avium* ATCC 25291^T; 3, *M. intracellulare* ATCC 13950^T; 4, strain KUM 060204^T; 5, strain NTH 512-121; 6, strain AHM 060905. MA, Mycolic acid.

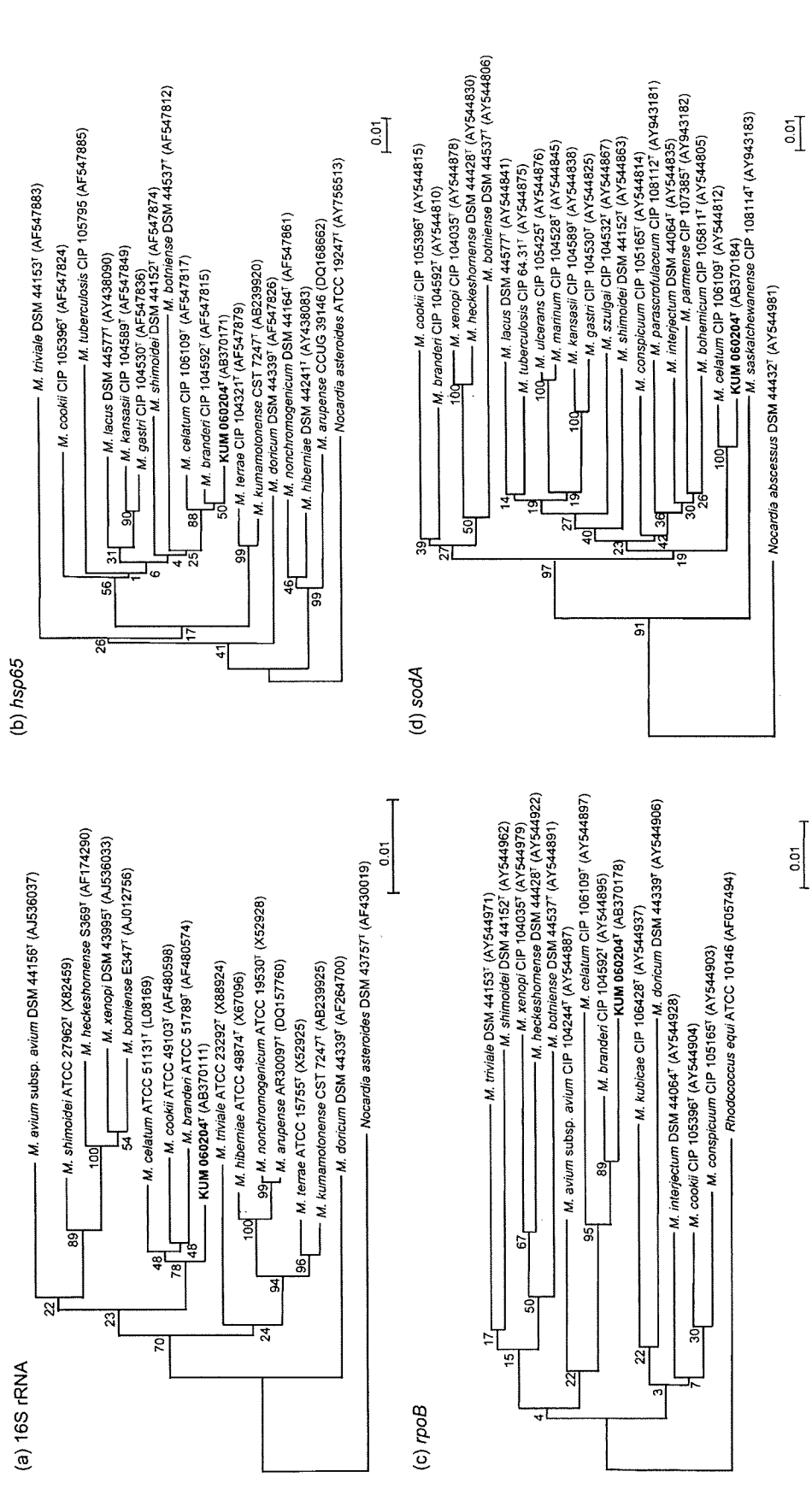

Fig. 2. Phylogenetic trees for isolate KUM 060204^T and closely related type strains of other mycobacterial species based upon comparisons of (a) 16S rRNA, (b) *hsp65*, (c) *rpoB* and (d) *sodA* gene sequences using the neighbour-joining method. The trees were rooted using the sequences of *Nocardia asteroides* (16S rRNA and *hsp65*), *Rhodococcus equi* (*rpoB*) and *Nocardia abscessus* (*sodA*) as the outgroups. The scale bars represent a 1 % sequence difference.

Table 4. Levels of DNA–DNA relatedness between strain KUM 060204^T and related *Mycobacterium* species

Strain	Similarity value (%) with labelled DNA from:			
	KUM 060204^T	*M. celatum* ATCC 51131^T	*M. branderi* ATCC 51789^T	*M. branderi* ATCC 51788
KUM 060204^T	100	49.1	46.0	47.6
M. celatum ATCC 51131^T	49.9	100	62.4	59.8
M. branderi ATCC 51789^T	44.5	51.3	100	100
M. branderi ATCC 51788	41.5	46.2	92.5	100

tol, but resistant to isoniazid and rifampicin. Sequence analysis of the 16S rRNA, *hsp65*, *rpoB* and *sodA* genes indicated that *M. kyorinense* is a mycobacterial species most closely related to *M. celatum* and *M. branderi*. DNA–DNA hybridization revealed that *M. kyorinense* exhibits DNA similarity values below the suggested threshold with its phylogenetic neighbours *M. celatum* ATCC 51131^T, *M. branderi* ATCC 51789^T and *M. branderi* ATCC 51788 (similarity 49.9, 44.5 and 41.5 %, respectively), thus defining it as a distinct species. *M. kyorinense* was placed in the slow-growing mycobacteria group.

The type strain is KUM 060204^T (=JCM 15038^T=DSM 45166^T), isolated from sputum in a patient with pneumonia.

ACKNOWLEDGEMENTS

This work was supported by grants from the Ministry of Health, Labour and Welfare (Research on Emerging and Re-emerging Infectious Diseases, Health Sciences Research Grants) of Japan, The Japan Health Sciences Foundation, Ministry of Education Culture Sports Science and Technology, and The United States–Japan Cooperative Medical Science Program against Tuberculosis and Leprosy.

REFERENCES

Boor, K. J., Duncan, M. L. & Price, C. W. (1995). Genetic and transcriptional organization of the region encoding the beta subunit of *Bacillus subtilis* RNA polymerase. *J Biol Chem* **270**, 20329–20336.

Brander, E., Jantzen, E., Huttunen, R., Julkunen, A. & Katila, M. L. (1992). Characterization of a distinct group of slowly growing mycobacteria by biochemical tests and lipid analyses. *J Clin Microbiol* **30**, 1972–1975.

Brown-Elliott, B. & Wallace, R. J., Jr (2005). Infections caused by nontuberculous mycobacteria. In *Principles and Practice of Infectious Diseases*, vol. 2, pp. 2909–2915. Edited by G. L. Mandell, J. E. Bennett & R. Dolin. Pennsylvania: Elsevier.

Butler, W. R., O'Connor, S. P., Yakrus, M. A., Smithwick, R. W., Plikaytis, B. B., Moss, C. W., Floyd, M. M., Woodley, C. L., Kilburn, J. O. & other authors (1993). *Mycobacterium celatum* sp. nov. *Int J Syst Bacteriol* **43**, 539–548.

Chapin, K. C. (2007). Principles of stains and media. In *Manual of Clinical Microbiology*, 9th edn, pp. 182–191. Edited by P. R. Murray, E. J. Baron, M. L. Landry, J. H. Jorgensen & M. A. Pfaller. Washington, DC: American Society for Microbiology.

Domenech, P., Jimenez, M. S., Menendez, M. C., Bull, T. J., Samper, S., Manrique, A. & Garcia, M. J. (1997). *Mycobacterium mageritense* sp. nov. *Int J Syst Bacteriol* **47**, 535–540.

Ezaki, T., Hashimoto, Y., Takeuchi, N., Yamamoto, H., Liu, S. L., Miura, H., Matsui, K. & Yabuuchi, E. (1988). Simple genetic method to identify viridans group streptococci by colorimetric dot hybridization and fluorometric hybridization in microdilution wells. *J Clin Microbiol* **26**, 1708–1713.

Ezaki, T., Hashimoto, Y. & Yabuuchi, E. (1989). Fluorometric deoxyribonucleic acid–deoxyribonucleic acid hybridization in micro-dilution wells as an alternative to membrane filter hybridization in which radioisotopes are used to determine genetic relatedness among bacterial strains. *Int J Syst Evol Microbiol* **39**, 224–229.

Kent, P. T. & Kubica, G. P. (1985). *Public Health Mycobacteriology: a Guide for the Level III Laboratory*. Atlanta: US Department of Health and Human Services, Centers for Disease Control.

Kirschner, P., Springer, B., Vogel, U., Meier, A., Wrede, A., Kiekenbeck, M., Bange, F. C. & Bottger, E. C. (1993). Genotypic identification of mycobacteria by nucleic acid sequence determination: report of a 2-year experience in a clinical laboratory. *J Clin Microbiol* **31**, 2882–2889.

Koukila-Kahkola, P., Springer, B., Bottger, E. C., Paulin, L., Jantzen, E. & Katila, M. L. (1995). *Mycobacterium branderi* sp. nov., a new potential human pathogen. *Int J Syst Bacteriol* **45**, 549–553.

Li, Y., Kawamura, Y., Fujiwara, N., Naka, T., Liu, H., Huang, X., Kobayashi, K. & Ezaki, T. (2004). *Sphingomonas yabuuchiae* sp. nov. and *Brevundimonas nasdae* sp. nov., isolated from the Russian space laboratory Mir. *Int J Syst Evol Microbiol* **54**, 819–825.

Masaki, T., Ohkusu, K., Hata, H., Fujiwara, N., Iihara, H., Yamada-Noda, M., Nhung, P. P., Hayashi, M., Asano, Y. & other authors (2006). *Mycobacterium kumamotonense* sp. nov. recovered from clinical specimen and the first isolation report of *Mycobacterium arupense* in Japan: novel slowly growing, nonchromogenic clinical isolates related to *Mycobacterium terrae* complex. *Microbiol Immunol* **50**, 889–897.

Medical Section of the American Lung Association (1997). Diagnosis and treatment of disease caused by nontuberculous mycobacteria. This official statement of the American Thoracic Society was approved by the Board of Directors, March 1997. *Am J Respir Crit Care Med* **156**, S1–S25.

NCCLS (2003). *Susceptibility Testing of Mycobacteria, Nocardiae, and Other Aerobic Actinomycetes; Approved Standard*. NCCLS document M24-A. Wayne, PA: National Committee for Clinical Laboratory Standards.

Telenti, A., Marchesi, F., Balz, M., Bally, F., Bottger, E. C. & Bodmer, T. (1993). Rapid identification of mycobacteria to the species level by polymerase chain reaction and restriction enzyme analysis. *J Clin Microbiol* **31**, 175–178.

Vincent, V. & Gutierres, M. C. (2007). Mycobacterium: laboratory characteristics of slowly growing mycobacteria. In *Manual of Clinical Microbiology*, 9th edn, pp. 573–588. Edited by P. R. Murray, E. J. Baron, M. L. Landry, J. H. Jorgensen & M. A. Pfaller. Washington, DC: American Society for Microbiology.

Biochemical and Biophysical Research Communications 387 (2009) 272–277

Contents lists available at ScienceDirect

Biochemical and Biophysical Research Communications

journal homepage: www.elsevier.com/locate/ybbrc

Dissection of Rab7 localization on *Mycobacterium tuberculosis* phagosome

Shintaro Seto [a], Sohkichi Matsumoto [b], Isamu Ohta [c], Kunio Tsujimura [a], Yukio Koide [a,*,1]

[a] Department of Infectious Diseases, Hamamatsu University School of Medicine, 1-20-1 Handa-yama, Higashi-ku, Hamamatsu 431-3192, Japan
[b] Department of Bacteriology, Osaka City University Graduate School of Medicine, 1-4-3 Asahi-machi, Abeno-ku, Osaka 545-8585, Japan
[c] Research Equipment Center, Hamamatsu University School of Medicine, 1-20-1 Handa-yama, Higashi-ku, Hamamatsu 431-3192, Japan

ARTICLE INFO

Article history:
Received 16 June 2009
Available online 4 July 2009

Keywords:
Macrophage
Mycobacterium tuberculosis
Rab7
Phagosome maturation
Phagolysosome biogenesis

ABSTRACT

The late endosomal marker Rab7 has been long believed to be absent from the phagosome containing *Mycobacterium tuberculosis* (*M.tb*) in macrophage, but the detail kinetics remains elusive. Here, we found that Rab7 is transiently recruited to and subsequently released from *M.tb* phagosomes. For further understanding of the effect of Rab7 dissociation from the phagosome, we examined the localization of lysosomal markers on the phagosome in the macrophage expressing a dominant-negative Rab7. The localization of lysosomal associated membrane protein-2 (LAMP-2) on the phagosome was Rab7-independent, while that of cathepsin D was Rab7-dependent. These results agree with the localization of each lysosomal marker on *M.tb* phagosome at 6 h postinfection-*i.e.*, LAMP-2, but not cathepsin D localized on the majority of *M.tb* phagosomes. These results suggest that the dissociation of Rab7 from *M.tb* phagosome is the important process in inhibition of phagolysosome biogenesis.

Introduction

Engulfment of pathogens by macrophages is an important initial step in the innate immune response. Pathogens phagocytosed by macrophages are enclosed into phagocytic vacuoles and processed by a series of interactions with endosome vesicles. This well-known process is called phagosome maturation. During the maturation process, phagosomes acquire degradative and microbicidal properties and undergo phagolysosome biogenesis by fusing with lysosomes. Several proteins, including Rab GTPase proteins, play pivotal roles in phagosome maturation and phagolysosome biogenesis [1]. Rab5 is associated with early phagosomes followed by recruitment of its effector proteins EEA1 and Class III phosphatidylinositol 3-kinase [2]. Rab7 appears on the phagosome membrane after Rab5 dissociation and resides there during the subsequent phagosome maturation [3]. Rab7 regulates the transportation and fusion of late endosomes and lysosomes [1] and has been implicated in the interaction between phagosomes and late endosomal compartments [4].

Mycobacterium tuberculosis (*M.tb*) is a causative pathogen of tuberculosis and has the ability to survive and proliferate in macrophages by blocking phagolysosome biogenesis [5,6]. In the current model of *M.tb*-induced inhibition of phagolysosome biogenesis, phagosome maturation is arrested at the stage of Rab5-Rab7 conversion [7] on *M.tb* phagosomes, leading to the inhibition of phagolysosome biogenesis [8]. This hypothesis is supported by observations that Rab7 is absent from mycobacterial phagosomes in macrophages [9,10]. However, the model was challenged by an observation that *M.tb* phagosomes are associated with lysosomal markers in the early stage of infection, suggesting that *M.tb* phagosomes fuse with lysosomes [11]. These conflicting observations indicate that more precise studies are necessary, particularly studies focusing on the kinetics of Rab7 localization during *M.tb*-induced inhibition of phagolysosome biogenesis. We therefore investigated the temporal and spatial localization of Rab7 in *M.tb*-infected macrophages, together with that of lysosomal markers, lysosomal associated membrane protein-2 (LAMP-2) and cathepsin D. In this study, we demonstrated that Rab7 is transiently recruited to *M.tb* phagosome, after which *M.tb* promotes the dissociation of Rab7 from the phagosome, suggesting that the dissociation of Rab7 limits the subsequent recruitment of cathepsin D and results in the blocking of phagolysosome biogenesis.

Materials and methods

Cell and bacterial cultures. Raw264.7 macrophage was obtained from the American Type Culture Collection and maintained in Dulbecco's modified Eagle's medium (DMEM; Sigma–Aldrich) supplemented with 10% fetal bovine serum (FBS; Thermo Trace), 25 μg/ml penicillin G, and 25 μg/ml streptomycin at 37 °C under 5% CO_2. *M. tuberculosis* H37Rv was grown to mid-logarithmic phase in 7H9 medium supplemented with 10% Middlebrook ADC (BD Bio-

* Corresponding author. Fax: +81 53 435 2101.
E-mail address: koidelb@hama-med.ac.jp (Y. Koide).
[1] Address: Executive director, Hamamatsu University School of Medicine, 1-20-1 Handa-Yama, Higashi-ku, Hamamatsu 431-3192, Japan

0006-291X/$ - see front matter © 2009 Elsevier Inc. All rights reserved.
doi:10.1016/j.bbrc.2009.06.152

sciences), 0.5% glycerol and 0.05% Tween 80 (*Mycobacterium* complete medium) at 37 °C. *M.tb* transformed with a plasmid encoding DsRed [12] was grown in *Mycobacterium* complete medium containing 25 μg/ml kanamycin. *Staphylococcus aureus* was grown in brain heart infusion broth (BD Biosciences) at 37 °C.

Antibodies. Rabbit anti-Rab7 polyclonal antibody (Sigma–Aldrich), rat anti-mouse LAMP-2 monoclonal antibody (SouthernBiotech), goat anti-mouse cathepsin D polyclonal antibody (R&D systems), rabbit anti-cytochrome C polyclonal antibody (Cell Signaling), mouse anti-GFP monoclonal antibody (TaKaRa Bio) were all purchased. Alexa488- and Alexa546-conjugated anti-IgG antibodies (Invitrogen) and 10-nm gold particle-conjugated anti-mouse IgG antibody (EY Laboratories) were purchased.

Plasmid constructs and transfection. Human Rab7 was amplified by PCR using cDNA derived from HeLa cells as a template and primers CAGATCTATGACCTCTAGGAAGAAAGTGTTGCTG and CGAATTCAGCAACTGCAGCTTTCTGCCG. PCR product of Rab7 was inserted into the pEGFP-C1 (Invitrogen). A constitutive-active and a dominant-negative Rab7 mutant were made by site-directed mutagenesis using the Quick-Change site-directed mutagenesis kit (Stratagene), as previously reported [13]. Three million Raw264.7 cells were transfected with 15 μg of plasmid DNA using an MP-100 electroporator (Digital Bio Technology) according to the manufacturer's instructions. Transfected cells were incubated in DMEM with 10% FBS for 24 h before the start of experiments.

Infection of bacteria. Transfected cells grown on round coverslips in 12-well plates were infected with bacteria. Bacterial cells were washed with PBS containing 0.05% Tween 80 three times and suspended in DMEM with 10% FBS at a multiplicity of infection (MOI) of 10–30. Aliquots of 1 ml of bacterial suspension were added to transfected Raw264.7 cells on coverslips in 12-well plates, followed by centrifugation at 150g for 5 min and incubation for 10 min at 37 °C. Infected cells on coverslips were washed with DMEM three times to remove non-infected bacteria, and then incubated with DMEM containing 10% FBS. At the indicated time points, infected cells were fixed with 1% or 3% paraformaldehyde in PBS.

Confocal microscopy. Imaging of cells was performed with a CSU LiveStage LS-1 confocal microscope system (Yokogawa). Four-dimensional (4D) live microscopy was performed with a CSU LiveStage LS-1 confocal microscope system as described previously [14] with modifications. Transfected Raw264.7 cells grown on a 35-mm glass base dish were infected with *M.tb* expressing DsRed. Synchronous infection was performed with centrifugation, washing with DMEM, and incubation with DMEM containing 10% FBS and 20 mM HEPES (pH7.3) without phenol red. Temperature control of the infected cells was carried out by an Onpu-4 incubation system (Taiei-denki). Serial confocal sections (1.5 μm) within a z-stack spanning a total thickness of 20 μm were taken every 5 min from 30 to 155 min after infection. Images with infected bacteria in transfected macrophage cells were chosen from the z-stacks at each time point to make a time-lapse sequence.

Immunoelectron microscopy. M.tb-infected macrophages were fixed with 3% paraformaldehyde and 0.1% glutaraldehyde in PBS overnight at 4 °C. Dehydration was carried out with a series of ethanol washes. Samples were embedded in LR White resin (OKEN) according to the manufacturer's protocol. Thin sections were cut with diamond knives and mounted on nickel grids. The sections were blocked with 3% BSA in PBS for 30 min. Sections were then incubated with anti-GFP antibody (1:30 v/v) in PBS containing 1% BSA overnight at 4 °C, followed by incubation with 10-nm gold-particle-conjugated secondary antibody (1:30 v/v) for 1 h at room temperature. Samples on grids were counter stained with 2% (wt/vol) uranyl acetate and then observed with a JEM-1220 electron microscope (JEOL). Image J was used to quantify the gold particles and the area of phagosomes.

Isolation of microbead and M.tb phagosomes. Six 15-cm plates of Raw264.7 cells were used for each condition. For isolation of the microbead phagosomal fraction, microbeads (2 μm, Polyscience) were added to Raw264.7 cells for 1 h, washed three times with prewarmed DMEM and incubated in DMEM with 10% FBS for the indicated times. Raw264.7 cells were then collected, lysed, and subjected to discontinuous sucrose gradient centrifugation as described previously [4]. For isolation of the *M.tb* phagosomal fraction, bacteria at an MOI of 10–30 were added to Raw264.7 cells in DMEM with 10% FBS for 1 h, washed and then incubated for the indicated times. Infected cells were collected, lysed, and subjected to fractionation as described previously [15]. For immunoblotting analysis, aliquots of 12.5 μg of Raw264.7 cell lysate and 3 μg of phagosomal fraction proteins were separated by SDS–polyacrylamide gel electrophoresis (PAGE) and then subjected to immunoblotting analysis using anti-Rab7 antibody (1:200 v/v), anti-LAMP-2 antibody (1:200 v/v), anti-cathepsin D antibody (1:200), and anti-cytochrome C (1:100 v/v). Band intensities from three independent experiments were quantified by Image J (http://rsb.info.nih.gov/ij/).

Immunofluorescence microscopy. Raw264.7 cells grown on round coverslips in 12-well plates were allowed to phagocytose microbeads or infected with bacteria for the indicated times, fixed with 3% paraformaldehyde in PBS for 1 h at room temperature, permeabilized with 0.1% Triton X-100 in PBS for 5 min, and finally washed with PBS. Fixed cells were blocked with 3% bovine serum albumin in PBS for 1 h followed by staining with the anti-LAMP-2 (1:50 v/v), cathepsin D (1:50 v/v) antibodies for 1 h, and then incubated with Alexa488- or Alexa546-conjugated anti-IgG antibodies (1:1000 v/v) for 1 h.

Statistics. The unpaired two-sided Student's *t*-test was used to assess the statistical significance of differences between the two groups.

Results and discussion

Rab7 transiently localizes on M.tb phagosome

Rab7 has been shown to be absent from mycobacterial phagosomes in macrophages at the time point when its recruitment generally occurs [9,10]. On the other hand, Clemens and Horwitz demonstrated that *M.tb* phagosomes acquired Rab7 in infected HeLa cells [16], and Sun et al. demonstrated the presence of Rab7 on *Mycobacterium bovis* Bacilus Calmette-Guérin phagosomes [17]. However, there are no crucial reports about the interaction between Rab7 and *M.tb* phagosomes in infected macrophages, especially the kinetics of Rab7 localization immediately after infection. We first examined the localization kinetics of Rab7 on the phagosomes in *M.tb*-infected macrophages. For this purpose, Raw264.7 macrophage cell line expressing enhanced GFP fused with Rab7 (EGFP-Rab7) was employed, because no satisfactory staining was obtained with the commercially available anti-Rab7 antibodies. Raw264.7 cells expressing EGFP-Rab7 were infected with *M.tb* expressing DsRed for 30 min or 6 h. Rab7 failed to localize on the majority of *M.tb* phagosomes at 6 h postinfection (Fig. 1B), although clear signals of EGFP-Rab7 was observed on the phagosomes at 30 min postinfection (Fig. 1A). The proportion of Rab7-positive phagosomes containing *M.tb* reached approximately 80% at 30 min postinfection, as observed in macrophages infected with *S. aureus*, and it decreased to about 30% by 6 h (Fig. 1C) and remained at this level until at least 12 h (data not shown). That of *S. aureus* retained more than 80% at 6 and 12 h postinfection (Fig. 1C and data not shown). Rab7 localized on about 75% of heat-inactivated *M.tb* phagosomes at 6 h after phagocytosis (Fig. 1D), suggesting that live *M.tb* actively promotes Rab7 dissociation from the phagosome.

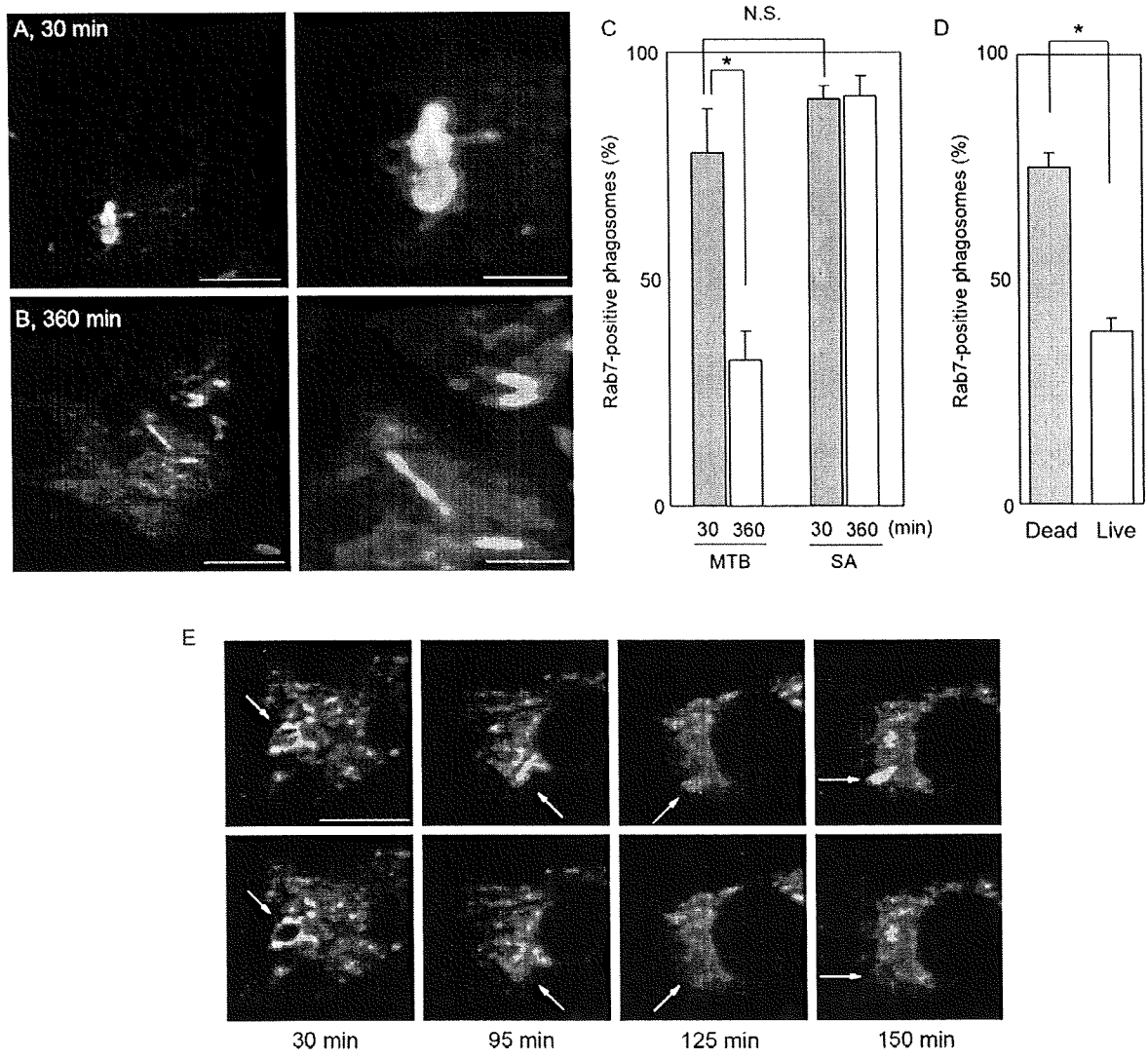

Fig. 1. Dynamics of Rab7 localization on *M.tb* phagosomes. (A, B) Raw264.7 cells expressing EGFP-Rab7 were infected with *M.tb* (MTB) expressing DsRed for 30 min (A) or 6 h (B). Cells were then fixed and observed with confocal microscopy. The right panels show the enlarged images of the phagosomes shown at left. Scale bar, 10 μm (left panel), 3 μm (right panel). (C) The proportion of Rab7-positive phagosomes containing *M.tb* (MTB) and *S. aureus* (SA) at 30 min and 6 h postinfection. (D) The proportion of Rab7-positive phagosomes containing live (Live) and heat-inactived (Dead) *M.tb* at 6 h postinfection. Data represent the average of three independent experiments in which more than 200 phagosomes were counted for each condition in (C) and (D). $^{*}P < 0.05$. N.S., no significance. (E) Raw264.7 cells expressing EGFP-Rab7 were infected with *M.tb* expressing DsRed and analyzed by 4D microscopy. The upper and lower panels show fluorescent images of the same Raw264.7 cell expressing EGFP-Rab7 (green) with or without fluorescent images of *M.tb* (red), respectively, at the indicated times after infection. Arrow indicates *M.tb* phagosome. Scale bar, 10 μm.

We investigated the dynamics of EGFP-Rab7 localization on *M.tb* phagosomes by live 4D confocal microscopy (Fig. 1E and Movie S1). At 30 min postinfection, Rab7 was clearly present on the *M.tb* phagosome. The outline of the Rab7 signal surrounding the phagosome began to fade at 95 min and disappeared completely at 125 min. At 150 min postinfection, Rab7 was still absent from the phagosome. These results suggest that Rab7 started to localize on the majority of *M.tb* phagosome immediately after infection, but viable *M.tb* subsequently caused the dissociation of Rab7 from the phagosome.

We applied immunoelectron microscopy to investigate Rab7 localization on *M.tb* phagosomes. Macrophages expressing EGFP-Rab7 were infected with *M.tb* for 30 min or 6 h, fixed and processed for immunoelectron microscopy using anti-GFP antibody. Gold particles forming clusters were associated with *M.tb* phagosome membranes at 30 min, but not at 6 h postinfection (Fig. 2A and B). Quantitative analysis revealed that about 80% of *M.tb* phagosomes is associated with gold particles forming clusters at 30 min and that the number of gold particles associated with *M.tb* phagosomes was remarkably decreased at 6 h (Fig. 2C). These results suggest that *M.tb* phagosomes acquire Rab7 molecules by the association with Rab7-containing vesicles immediately after infection, and that this association is canceled at the later stage of infection.

To confirm biochemically that Rab7 is transiently recruited to and then dissociated from *M.tb* phagosomes, we conducted immunoblotting analysis to detect Rab7 in isolated mycobacterial phagosomal fractions. Raw264.7 macrophages were allowed to phagocytose microbeads or infected with *M.tb* for 30 min or 6 h, and the phagosomal fractions were isolated as previously reported [4,15]. We checked the purity of phagosomes by thin-section electron microscopy and immunoblotting analysis for cytochrome C, and found that few organelles and materials had contaminated in both phagosomal fractions (Supplemental Fig. 1). As shown in Fig. 3, the amount of Rab7 on *M.tb* phagosomes at 6 h postinfection decreased significantly to 19 ± 7% (mean ± standard deviation,

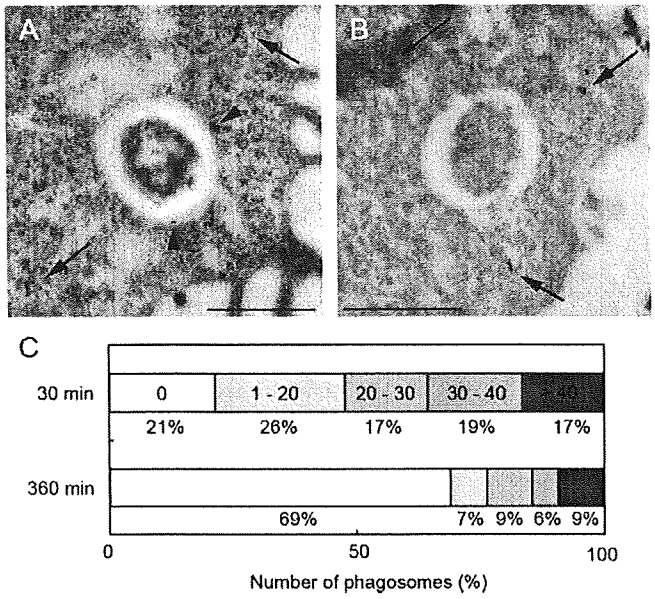

Fig. 2. Immunoelectron microscopic analysis of Rab7 localization on *M.tb* phagosomes. (A, B) Immunoelectron microscopic images of *M.tb*-infected macrophages. Raw264.7 macrophages expressing EGFP-Rab7 were infected with *M.tb* for 30 min (A) or 6 h (B) and processed for immunoelectron microscopy. Thin sections were stained with anti-GFP antibody followed by 10-nm gold-particle-conjugated secondary antibody. Arrow and arrowhead indicate gold particles forming clusters in the cytoplasmic region and on the phagosome, respectively. Scale bar, 0.5 μm. (C) Distribution of Rab7-gold particles associated with *M.tb* phagosomes. The number of gold particles on each *M.tb* phagosome in EGFP-Rab7-positive macrophages was counted at 30 min ($n = 52$ phagosomes) or 6 h ($n = 56$ phagosomes) postinfection, and the number per area (μm^2) of each phagosome was calculated. The distribution of the number of gold particles associated with the phagosome is indicated in the bar. The percentages of the different populations are shown at each time point.

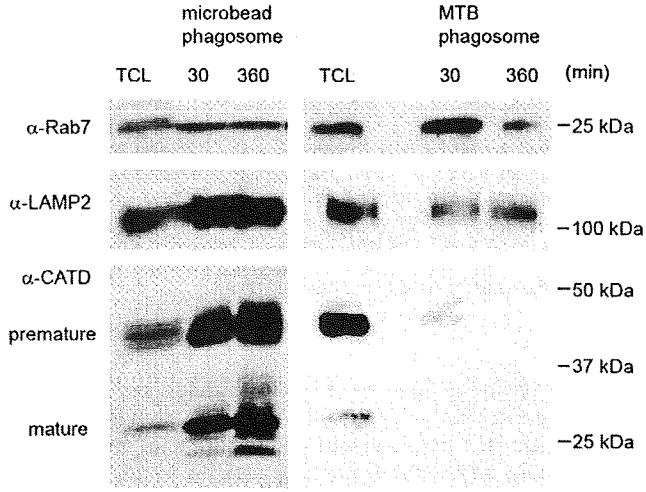

Fig. 3. Rab7 localization in isolated *M.tb* phagosomal fractions. Immunoblotting analysis of microbead and *M.tb* (MTB) phagosomal fractions with antibodies to Rab7, LAMP-2, and cathepsin D (CATD) is shown. Total cell lysates from Raw264.7 cells (TCL) and phagosomal fractions of microbead or *M.tb* were subjected to SDS–PAGE, followed by immunoblotting using indicated antibodies.

$n = 3$, $P < 0.05$) of that at 30 min, whereas the amounts on microbead phagosomes at 30 min and 6 h were nearly the same. These results are in line with those obtained by immunofluorescence and immunoelectron microscopic analyses and support the idea that Rab7 is transiently recruited to and then dissociated from *M.tb* phagosomes.

Localization of the constitutively active form of Rab7 on M.tb phagosome

It seems most likely that the dissociation of Rab7 from *M.tb* phagosomes is caused by *M.tb*-mediated conversion of its form from the GTP-bound type to the GDP-bound one. To investigate the mechanism by which Rab7 is released from *M.tb* phagosomes after transient recruitment, we employed the constitutive-active Rab7 mutant Rab7Q67L which lacks GTPase activity [18]. EGFP-fused Rab7Q67L localized on the majority of *M.tb* phagosomes at 30 min postinfection, and were dissociated from phagosomes at 6 h (data not shown), just as for the wild type of Rab7 (Fig. 1). These results suggest that the GTPase activity of Rab7 is not required for the dissociation of Rab7 from *M.tb* phagosomes. We propose two possibilities to account for the GTPase-independent dissociation of Rab7 from *M.tb* phagosomes. First, Rab7 dissociation is caused by the inactivation of the tethering and/or docking molecules of Rab7 to *M.tb* phagosome, which leads to the increase of Rab7 efflux from the phagosome. Second, vesicles containing Rab7 are transiently associated with and then dissociated from *M.tb* phagosomes at the early and late stages of infection, respectively, as shown by immunoelectron microscopy (Fig. 2).

Localization of lysosomal proteins on M.tb phagosome

To further understand the effect of Rab7 dissociation from the phagosome, we examined that lysosomal marker proteins depend on the function of Rab7 to localize on the phagosome (Fig. 4). We chose LAMP-2 and cathepsin D that have been shown to reside on microbead phagosome [19] as the lysosomal markers. Raw264.7 macrophages simultaneously transfected with two plasmids encoding EGFP and a dominant-negative form of Rab7, Rab7T22N, were allowed to phagocytose microbeads for 2 h and then stained with anti-LAMP-2 or anti-cathepsin D antibodies. In the wild type Raw264.7 cells, both lysosomal markers are localized on more than 80% of microbead phagosomes at 2 h after phagocytosis (data not shown). In Raw264.7 cells expressing Rab7T22N, LAMP-2 was recruited to microbead phagosomes (Fig. 4A), while cathepsin D was not (Fig. 4B). The results indicate that LAMP-2 on the phagosome is Rab7-independent, while that of cathepsin D is Rab7-dependent.

Both LAMP-2 and cathepsin D showed limited localizations on mycobacterial phagosomes in macrophages 24 h after infection and later [6]. However, the kinetics of their localization on mycobacterial phagosomes immediately after infection is not known. We therefore examined the localization of LAMP-2 and cathepsin D on *M.tb* phagosomes by immunofluorescence microscopy (Fig. 4). LAMP-2 localized on about 80% and 60% of *M.tb* phagosomes at 30 min and 6 h postinfection, respectively (Fig. 4C and D). Cathepsin D localized on about 50% of phagosomes at 30 min postinfection, but its localization on *M.tb* phagosome showed a punctuated staining pattern (Fig. 4E). At 6 h postinfection, it was not present on most *M.tb* phagosomes (Fig. 4F).

Localization of LAMP-2 and cathepsin D on isolated *M.tb* phagosomes was examined by immunoblotting analysis (Fig. 3C). Both lysosomal markers were present in the microbead phagosomal fractions, as previously reported [19]. In the *M.tb* phagosomal fractions, LAMP-2 was present, but cathepsin D was absent at 30 min and 6 h postinfection. The results obtained by immunofluorescence microscopic and immunoblotting analyses suggest that LAMP-2 localizes on the major proportion of *M.tb* phagosomes and that cathepsin D associates with *M.tb* phagosome immediately after infection, but the fusion of cathepsin D with *M.tb* phagosome is inhibited.

In conclusion, we propose the following model for *M.tb*-induced inhibition of phagolysosome biogenesis based on the data pre-

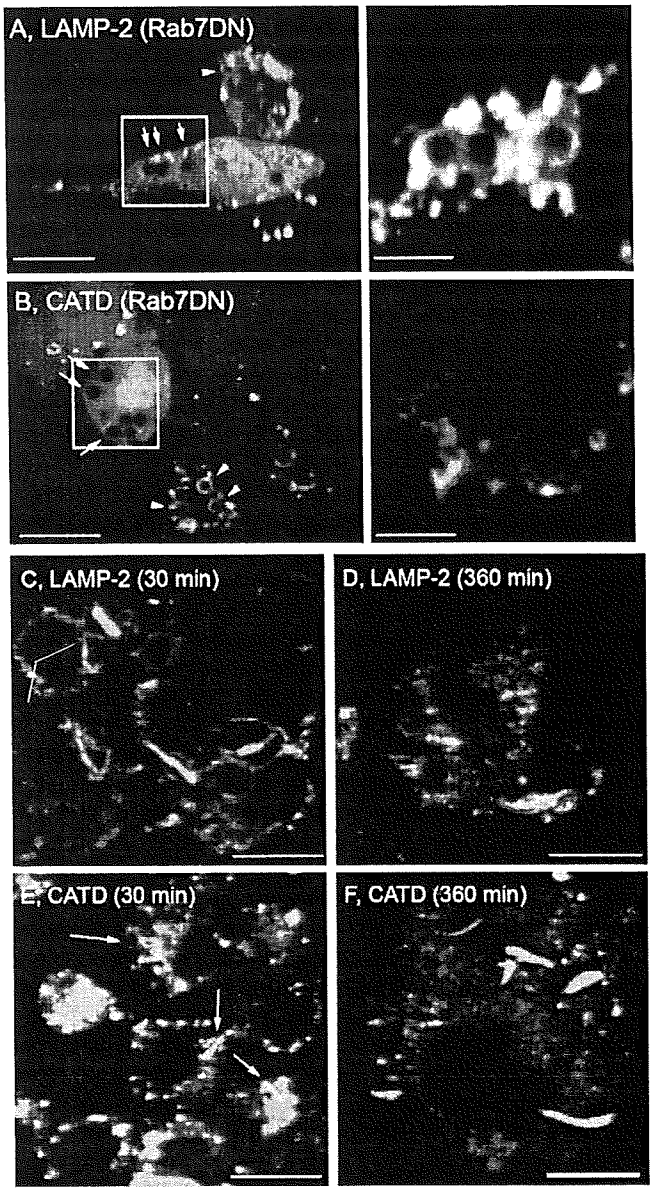

Fig. 4. Localization of lysosomal markers on *M.tb* phagosome. (A, B) Localization of LAMP-2 and cathepsin D (CATD) on microbead phagosomes in the macrophage expressing a dominant-negative form of Rab7. Raw264.7 cells transfected with two plasmids expressing EGFP and Rab7T22N, were allowed to phagocytose microbeads for 2 h. Cells were fixed, stained with anti-LAMP-2 and anti-CATD antibodies, and observed with confocal microscopy. Localization of LAMP-2 (A) and CATD (B) is shown. Arrows and arrowheads indicate the phagosomes in macrophages with and without expressing Rab7T22N, respectively. The right panels show the enlarged images of the phagosomes shown at left. Scale bar, 10 μm (left), 3 μm (right). (C–F) Localization of LAMP-2 and cathepsin D on *M.tb* phagosomes. Raw264.7 cells were infected with *M.tb* expressing DsRed for 30 min (C, E) or 6 h (D, F). Infected cells were fixed, stained with anti-LAMP-2 and anti-CATD antibodies, and observed with confocal microscopy. Localization of LAMP-2 (C, D) and CATD (E, F) is shown. Scale bar, 10 μm.

sented in this study. Early *M.tb* phagosomes can potentially fuse with late endosomes and lysosomes. However, viable *M.tb* has the ability to release Rab7 from the phagosome, resulting in the inhibition of the fusion with late endosomal and lysosomal vesicles. *M.tb* phagosomes are associated with LAMPs derived from the plasma membrane and the Golgi complex [20]. Alternatively, LAMPs are derived from the endocytic vesicles, which can fuse with the phagosome in the Rab7-independent manner. Vesicles containing cathepsin D is associated with *M.tb* phagosomes immediately after infection, but the fusion is inhibited by the uncharacterized mechanism. At the later infection, cathepsin D is not associated with the phagosomes, because dissociation of Rab7 causes the inhibition of fusion of *M.tb* phagosome with cathepsin D. Rab7 dissociation from the *M.tb* phagosome causes the blocking of subsequent phagosome maturation and phagolysosome biogenesis.

Acknowledgments

We thank Drs. Toshi Nagata and Masato Uchijima of Hamamatsu University School of Medicine for their helpful discussion. *M. tuberculosis* H37Rv was kindly provided by Dr. Isamu Sugawara of Research Institute of Tuberculosis in Tokyo. This work was supported by Grants-in-Aid for Scientific Research and COE Research from the Ministry of Education, Culture, Sports, Science and Technology of Japan; by Health and Labour Science Research Grants for Research into Emerging and Reemerging Infectious Diseases from the Ministry of Health, Labour and Welfare of Japan; and by the United States-Japan Cooperative Medical Science Committee.

Appendix A. Supplementary data

Supplementary data associated with this article can be found, in the online version, at doi:10.1016/j.bbrc.2009.06.152.

References

[1] O.V. Vieira, R.J. Botelho, S. Grinstein, Phagosome maturation: aging gracefully, Biochem. J. 366 (2002) 689–704.
[2] O.V. Vieira, R.J. Botelho, L. Rameh, S.M. Brachmann, T. Matsuo, H.W. Davidson, A. Schreiber, J.M. Backer, L.C. Cantley, S. Grinstein, Distinct roles of class I and class III phosphatidylinositol 3-kinases in phagosome formation and maturation, J. Cell Biol. 155 (2001) 19–25.
[3] O.V. Vieira, C. Bucci, R.E. Harrison, W.S. Trimble, L. Lanzetti, J. Gruenberg, A.D. Schreiber, P.D. Stahl, S. Grinstein, Modulation of Rab5 and Rab7 recruitment to phagosomes by phosphatidylinositol 3-kinase, Mol. Cell. Biol. 23 (2003) 2501–2514.
[4] M. Desjardins, L.A. Huber, R.G. Parton, G. Griffiths, Biogenesis of phagolysosomes proceeds through a sequential series of interactions with the endocytic apparatus, J. Cell Biol. 124 (1994) 677–688.
[5] J.A. Armstrong, P.D. Hart, Response of cultured macrophages to *Mycobacterium tuberculosis*, with observations on fusion of lysosomes with phagosomes, J. Exp. Med. 134 (1971) 713–740.
[6] D.L. Clemens, M.A. Horwitz, Characterization of the *Mycobacterium tuberculosis* phagosome and evidence that phagosomal maturation is inhibited, J. Exp. Med. 181 (1995) 257–270.
[7] J. Rink, E. Ghigo, Y. Kalaidzidis, M. Zerial, Rab conversion as a mechanism of progression from early to late endosomes, Cell 122 (2005) 735–749.
[8] I. Vergne, J. Chua, S.B. Singh, V. Deretic, Cell biology of mycobacterium tuberculosis phagosome, Annu. Rev. Cell Dev. Biol. 20 (2004) 367–394.
[9] L.E. Via, D. Deretic, R.J. Ulmer, N.S. Hibler, L.A. Huber, V. Deretic, Arrest of mycobacterial phagosome maturation is caused by a block in vesicle fusion between stages controlled by rab5 and rab7, J. Biol. Chem. 272 (1997) 13326–13331.
[10] V.A. Kelley, J.S. Schorey, *Mycobacterium*'s arrest of phagosome maturation in macrophages requires Rab5 activity and accessibility to iron, Mol. Biol. Cell 14 (2003) 3366–3377.
[11] N. van der Wel, D. Hava, D. Houben, D. Fluitsma, M. van Zon, J. Pierson, M. Brenner, P.J. Peters, *M. Tuberculosis* and *M. leprae* translocate from the phagolysosome to the cytosol in myeloid cells, Cell 129 (2007) 1287–1298.
[12] K. Aoki, S. Matsumoto, Y. Hirayama, T. Wada, Y. Ozeki, M. Niki, P. Domenech, K. Umemori, S. Yamamoto, A. Mineda, M. Matsumoto, K. Kobayashi, Extracellular mycobacterial DNA-binding protein 1 participates in mycobacterium-lung epithelial cell interaction through hyaluronic acid, J. Biol. Chem. 279 (2004) 39798–39806.
[13] C. Bucci, P. Thomsen, P. Nicoziani, J. McCarthy, B. van Deurs, Rab7: a key to lysosome biogenesis, Mol. Biol. Cell 11 (2000) 467–480.
[14] J. Chua, V. Deretic, *Mycobacterium tuberculosis* reprograms waves of phosphatidylinositol 3-phosphate on phagosomal organelles, J. Biol. Chem. 279 (2004) 36982–36992.
[15] W.L. Beatty, E.R. Rhoades, D.K. Hsu, F.T. Liu, D.G. Russell, Association of a macrophage galactoside-binding protein with *Mycobacterium*-containing phagosomes, Cell. Microbiol. 4 (2002) 167–176.
[16] D.L. Clemens, B.Y. Lee, M.A. Horwitz, *Mycobacterium tuberculosis* and *Legionella pneumophila* phagosomes exhibit arrested maturation despite acquisition of Rab7, Infect. Immun. 68 (2000) 5154–5166.

[17] J. Sun, A.E. Deghmane, H. Soualhine, T. Hong, C. Bucci, A. Solodkin, Z. Hmama, *Mycobacterium bovis* BCG disrupts the interaction of Rab7 with RILP contributing to inhibition of phagosome maturation, J. Leukoc. Biol. 82 (2007) 1437–1445.
[18] S. Meresse, J.P. Gorvel, P. Chavrier, The rab7 GTPase resides on a vesicular compartment connected to lysosomes, J. Cell Sci. 108 (Pt 11) (1995) 3349–3358.
[19] J. Garin, R. Diez, S. Kieffer, J.F. Dermine, S. Duclos, E. Gagnon, R. Sadoul, C. Rondeau, M. Desjardins, The phagosome proteome: insight into phagosome functions, J. Cell Biol. 152 (2001) 165–180.
[20] S. Obermuller, C. Kiecke, K. von Figura, S. Honing, The tyrosine motifs of Lamp 1 and LAP determine their direct and indirect targetting to lysosomes, J. Cell Sci. 115 (2002) 185–194.

Jpn. J. Infect. Dis., 62, 182-186, 2009

Original Article

Mycobacterium avium Complex Organisms Predominantly Colonize in the Bathtub Inlets of Patients' Bathrooms

Yukiko Nishiuchi*, Aki Tamaru[1], Seigo Kitada[2], Takahiro Taguri[2], Sohkichi Matsumoto[3], Yoshitaka Tateishi[2,3], Mamiko Yoshimura[3], Yuriko Ozeki[3], Narumi Matsumura[2], Hisashi Ogura[4], and Ryoji Maekura[2]

Toneyama Institute for Tuberculosis Research Osaka City University Medical School, Osaka 560-8552; [1]Department of Infectious Diseases, Osaka Prefectural Institute of Public Health, Osaka 537-0025; [2]National Hospital Organization Toneyama National Hospital, Osaka 560-8552; and [3]Department of Bacteriology and [4]Department of Virology, Osaka City University Graduate School of Medicine, Osaka 545-8585, Japan

(Received February 12, 2009. Accepted March 27, 2009)

SUMMARY: Medical treatment of pulmonary *Mycobacterium avium* complex (MAC) disease does not always provide curative effects and is frequently hampered by recurrence. This suggests the presence of a reservoir for MAC in the environment surrounding patients. We previously reported the recovery of MAC isolates from the residential bathrooms of outpatients. In the present study, to ascertain the colonizing sites and the possibility of an MAC reservoir in the bathrooms of patients, we tested the recovery and the genetic diversity of MAC isolates from 6 sites of specimens, including 2 additional sampling sites, inside the showerhead and the bathtub inlet, in the residential bathrooms of patients with pulmonary MAC disease. MAC isolates were recovered from 15 out of the 29 bathrooms (52%), including specimens from 14 bathtub inlets and 3 showerheads. Nearly half of these bathrooms (7/15) contained MAC strains that were identical or similar to their respective clinical isolates. Additionally, in 5 out of 15 bathrooms, polyclonal colonization was revealed by pulsed-field gel electrophoresis. The results imply that colonization of MAC organisms in the bathrooms of MAC patients occurs predominantly in the bathtub inlets, and there is thus a risk of infection and/or reinfection for patients via use of the bathtub and other sites in the bathroom.

INTRODUCTION

The incidence of pulmonary *Mycobacterium avium* complex (MAC) disease has increased over the past several decades (1-3). MAC disease occasionally leads to death even in patients without a history of lung diseases or immunodeficiency (2,4-6) and is characterized by multiple infection with genetically different strains (7,8). Although macrolide-based regimens are effective against MAC, the cure rate with these drugs is still low (56%) because patients drop out due to drug side effects, consecutive positive culture, and recurrence (2). Kobashi and Matsushima (9) reported that 41 of their 71 patients (58%) showed negative sputum cultures after successful completion of multidrug chemotherapy including a macrolide, and 16 of these 41 patients (39%) experienced recurrence. The genotyping research has demonstrated that patients with nodular bronchiectasis have multiple and/or repeated infections, and that frequent recurrence is due to reinfection with a genetically different strain or relapse with the original strain (7,8). To prevent recurrence of MAC disease, long-term treatment such as chemotherapy for 2 years (10) or 12-month treatment leading to culture-negative sputum (3) is recommended as a reasonable endpoint. The frequent recurrence and multiple infections suggest that polyclonal MAC colonization is likely to occur in the home environment surrounding patients with pulmonary MAC disease.

MAC is widely distributed both in the natural and living environment, and these environmental organisms are thought to be a source of infections (2,5). Drinking water systems are a possible source of disseminated MAC infection (11-16), which has been detected in biofilms of water distribution systems (13). In a recent study, we recovered MAC isolates from residential bathrooms but not from other sites within the residence (17). We also found that the appearance ratio in the bathrooms of patients with pulmonary MAC disease was significantly higher than that in the bathrooms of healthy volunteers ($P = 0.01$) (17). In the present study, therefore, we tried to determine the colonizing sites and to investigate the possibility of a reservoir of MAC organisms in the bathrooms of patients with MAC disease. We sampled specimens from 6 sites in the residential bathrooms of MAC-positive patients, including 2 sampling sites that were not included in our previous study: inside the showerhead and the bathtub inlet. A traditional Japanese bathtub has a water inlet below the water level, and we reasoned that biofilm produced by MAC organisms could develop inside this inlet, as well as within the showerheads. Finally, we examined the genetic diversity of the MAC isolates from specimens in the patients' bathrooms and sputa.

MATERIALS AND METHODS

Subjects and collection of samples: We collected 6 samples from the residential bathroom of each patient: 2 water samples (shower water and used bathtub water, 200 ml each), 3 scale samples (on the surface of the showerheads, inside

*Corresponding author: Mailing address: Toneyama Institute for Tuberculosis Research Osaka City University Medical School, 5-1-1 Toneyama, Toyonaka, Osaka 560-8552, Japan. Tel: +81-6-6853-5837, Fax: +81-6-6853-5839, E-mail: nishiuchi@med.osaka-cu.ac.jp

the showerhead, and inside the bathtub inlet), and 1 sample from the slime on the bathroom drain. Participants were outpatients diagnosed with pulmonary MAC disease ($n = 29$). All patients lived with their family and shared their bathroom with at least one other family member. Patients were diagnosed with pulmonary MAC disease according to the American Thoracis Society 1997 diagnostic criteria (18). Informed consent was obtained from all participants before the collection of samples. This study was approved by the Toneyama National Hospital institutional review board and complies with international guidelines for studies involving human subjects. Information regarding the bathrooms was collected by a questionnaire survey.

Culture of residential samples: The collected residential samples were cultured as described previously (17). In brief, water samples were centrifuged at 11,800 × g for 30 min at 4°C, and pellets from the shower water were suspended in 0.5 ml of phosphate buffer (PB) at pH 6.8, 200 μl of which was inoculated onto a Middlebrook 7H11-OADC agar plate containing the antibiotic mixture PANTA (7H11 PANTA plate). The pellet from the used bathtub water was treated with 3 ml of 2% sodium hydroxide solution for 10 min. After adding 6 ml of PB to this alkali-treated sample, it was centrifuged at 2,270 × g for 15 min, and resuspended in 0.5 ml of PB. The collected samples on the swabs were preincubated for 3 h at 25°C in a tryptic soy broth followed by alkali treatment, and the pellets were suspended in 1 ml of PB solution. One hundred to 200 μl of these suspensions were inoculated onto 7H11 PANTA plates at 37°C for 3 weeks. Growing colonies were examined microscopically, followed by Ziehl-Neelsen staining. The isolated acid-fast bacterial species were identified by the PCR method (19).

Genotypic analysis: Genotypic analyses were carried out using pulsed-field gel elecrophoresis (PFGE) as described previously (17). PFGE genotypic patterns were defined as follows: identical, when one case was not distinguishable from another; related, when the genotypic pattern differed by only 1-3 bands; and unrelated, when the genotypic pattern differed by 4 or more bands.

Statistical analysis: The chi-square and Mann-Whitney U-test were used for analysis. Findings of $P < 0.05$ were considered statistically significant, while those of $P < 0.1$ were considered as evidence of a statistical tendency.

RESULTS

Colonization of MAC in residential bathrooms: MAC isolates were frequently recovered from the residential bathrooms of outpatients with pulmonary MAC disease (Table 1). Twenty-nine bathrooms of patients were inspected in the present study, of which 15 and 1 were found to harbor *Mycobacterium avium* (52%) and *M. intracellulare* (3.4%), respectively. MAC isolates were recovered from 4 shower specimens in 3 bathrooms (3/29, 10%); the shower specimens were taken from the inside and surface of the showerheads, and from the shower water. MAC isolates were most frequently recovered from the scale of the bathtub inlets (14/25, 56%), though they were distributed throughout the bathroom (Table 1). In 7 specimens from bathtub inlets, more than 100 colonies of MAC were recovered from each primary isolation plate. The additional sampling sites were responsible for the increase in the recovery rate from 18% in our previous study (17) to 52% in the present study. In order to ascertain whether MAC continuously inhabits the inside of the showerheads and bathtub inlets, we took additional samples from these sites after an interval of 3 months in 2 bathrooms. MAC isolates were recovered from both sites (data not shown), indicating a long-lasting colonization of MAC at these sites.

Polyclonal MAC colonization: MAC isolates were recovered from more than 2 sampling sites in the bathrooms of 10 participants. Additionally, in some cases we obtained multiple isolates of MAC possessing a colony morphology different from that of the primary isolation plate. In order to clarify the genetic diversity of multiple MAC isolates from individual bathrooms, we analyzed the polymorphism of MAC isolates using PFGE (Fig. 1). In each of 5 bathrooms, we found multiple isolates that possessed different genotypic profiles. This demonstrated that polyclonal MAC colonization can occur within a single bathroom. In the case of patient #29 (P29), 5 MAC isolates were recovered from 3 different sampling sites, and they had 3 different PFGE profiles (Fig. 1). Interestingly, 3 MAC isolates from the bathtub inlet, each possessing a different colony morphology, also showed 3 different PFGE profiles. Similarly, unrelated genotypes of plural isolates recovered from 1 sampling site were observed in the cases of P8 and P17. These results indicate that polyclonal MAC strains are capable of growing together in the same location. In the case of P27, MAC isolates were recovered from 4 different sampling sites, and all of them had related PFGE profiles with 1-3 band differences (Fig. 1). Moreover, in the case of P9, 3 of 4 isolates which were recovered from 2 different sampling sites showed related PFGE profiles (Fig. 1). These related PFGE profiles reflect the genomic variation which may have occurred due to mutation of one of the strains.

Identical/related polymorphism between environmental and clinical isolates: To assess the relationship between the patient-derived clinical MAC isolates and the respective environmental isolates, we compared their polymorphism in

Table 1. Recovery of *M. avium* and *M. intracellulare* from residential bathrooms of outpatients with pulmonary MAC disease

	Sampling site						Total Sample (Residence)
	Surface of the shower head	Inside the shower head	Shower water	Bathtub inlet	Bathtub water	Drain	
No. of test samples	29	24	29	25	26	29	162 (29)
M. avium	1	2	1	14[1)]	7	7[2)]	32 (15)
M. intracellulare	0	0	0	0	0	1	1 (1)

Data are represented as the number of samples from which *M. avium* or *M. intracellulare* were recovered.
Numbers in parenthesis represent the number of residences.
[1)]: Over 100 colonies of *M. avium* in a primary isolation plate were recovered from 7 of 14 culture-positive samples.
[2)]: Over 100 colonies of *M. avium* in a primary isolation plate were recovereo from 2 of 7 culture-positive samples.

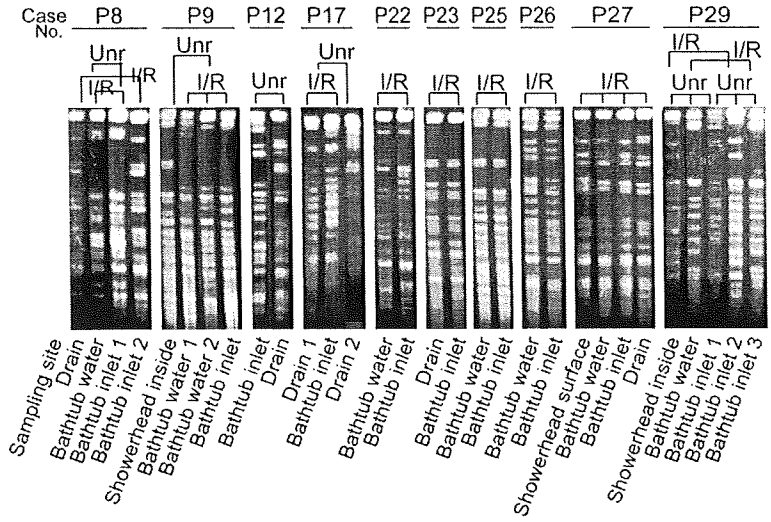

Fig. 1. Polyclonal colonization of *M. avium* complex (MAC) in residential bathrooms. Pulsed-field gel electrophoresis (PFGE) profiles of chromosomal *Xba*I digests of MAC isolates. Unr, unrelated profiles; I/R, identical or related profiles.

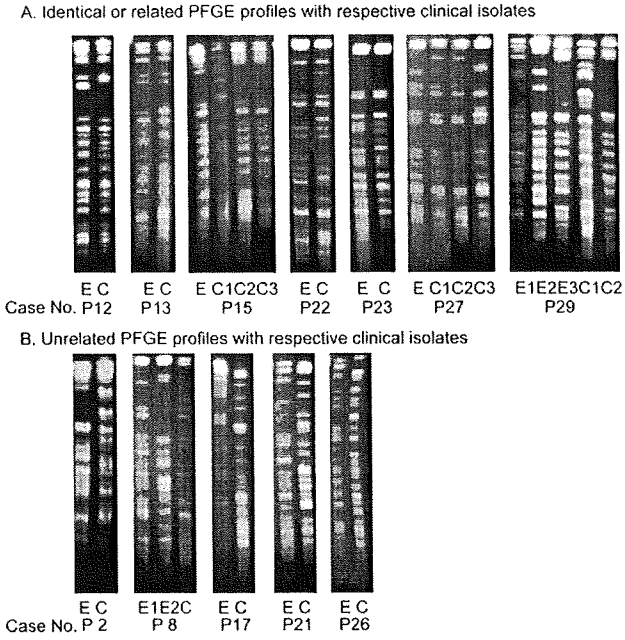

Fig. 2. Molecular typing of environmental and clinical *M. avium* complex (MAC) isolates. (A) Identical or related PFGE profiles of isolates from bathrooms with respective clinical isolates. E, environmental isolates; C, clinical isolates. C1 of P15, isolate from sputum 1 in December 2001; C2 of P15, isolate from sputum 2 in May 2003; C3 of P15, isolate from sputum 3 in January 2004; E of P27, isolate from bathtub inlet; C1 of P27, isolate from sputum 1 in December 2006; C2 of P27, isolate from sputum 2 in February 2007; C3 of P27, isolate from sputum 3 in July 2007; E1 of P29, isolates from bathtub inlet 1; E2 of P29, isolate from bathtub inlet 2; E3 of P29, isolate from bathtub inlet 3; C1 of P29, isolate from sputum 1 in June 2004; C2 of P29, isolate from sputum 2 in March 2006. (B) Unrelated PFGE profiles of isolates from bathrooms with respective clinical isolates. E1 of P8, isolate from drain; E2 of P8, isolate from bathtub inlet 1; E of P17, isolate from drain 2; E of P26, isolate from bathtub inlet.

individual cases. We recovered MAC in 15 cases, of which 11 and 1 cases were determined to contain *M. avium* isolates and *M. intracellulare* isolates, respectively, in both their environmental and clinical specimens. In the remaining 3 cases, *M. avium* isolates were recovered from the environment and *M. intracellulare* isolates were recovered from clinical specimens. Therefore, we compared the MAC genotypes in the former 12 cases. In 7 of 15 cases (47%), MAC isolates from the patients' bathrooms and their respective sputa had identical or related molecular profiles by PFGE anlysis (Fig. 2). In the other 5 cases, MAC isolates from the bathrooms possessed profiles different from those of their respective sputa (Fig. 2). These results are in agreement with our previous findings (17) that environmental isolates exhibit the identical polymorphism with their respective clinical isolates. The rate of identity obtained in the present study (47%, 7/15) is higher than that observed in the previous study (22%, 2/9) (17). We could compare the genetic diversity of retrospective sputum cultures in 3 cases. Genotypic analyses showed unrelated polymorphisms in 2 of these cases (Fig. 2, P15 and P29). The genotypes of the latent clinical strains were related to those of isolates from their respective bathrooms.

Bathtub types and bathroom maintenance: MAC bacilli appear to colonize in the bathroom preferentially over other household locations. However, no MAC isolates were recovered from half of the bathrooms examined in the present study. Therefore, to identify the risk factors for MAC colonization, we collected information regarding the type of bathtub and the method of maintaining the bathroom by a questionnaire survey. The characteristics of culture-negative versus culture-positive bathrooms are presented in Table 2. In the traditional Japanese bath, a bathtub inlet is installed inside the bathtub and below the water level. Some of the bathtub inlets are attached to the hot-water supply, while others are attached to the bath-boiler. MAC organisms are more likely to colonize in the bathtub inlet attached to the bath-boiler than in the inlet attached to the hot-water supply ($P < 0.01$, chi-square test). The bath-boiler can be classified into two types: a natural circulation type having two holes, an inlet and outlet, and a forced circulation type having one hole. In the present study, 8 participants used the natural circulation type of bath-boiler and all the bathtub inlets were found to retain MAC bacilli. In Japan, used bathtub water is sometimes reserved in the bathtub until the next day for washing clothes or to provide for a disaster such as an earthquake. MAC isolates were more frequently recovered from the samples taken from participants who were in a habit of reserving bathtub water; this relation reached the level of a tendency but was not statistically significant ($P = 0.09$, chi-square test). There was also a nonsignificant tendency for

Table 2. Participants' residential bathtub type and ventilation method of bathrooms

	Recovery of *M. avium* and *M. intracellulare*		
	Culture positive	Culture negative	Total
Type of bathtub			
Bathtub supplied with hot-water	3	10	13*
Bathtub attached to a bath-boiler			
Natural circulation type[1)]	8	0	8
Forced circulation type[2)]	4	4	8
The time of draining off water from bathtub after bathing			
Shortly after bathing	2	6	8**
Next day	12	8	20
Unknown	1	0	1
Ventilation of a bathroom			
Bathroom dryer	0	3	3**
Ventilating fan			
Regular use	0	1	1
1 - 8 h after bathing	2	2	4
0.5 - 1 h after bathing	3	2	5
No bathroom dryer or no ventilating fan	10	6	16

Data are represented as the number of residences.
[1)]: Natural circulation type of bath-boiler which has two holes in a bathtub.
[2)]: Forced ciculation type of bath-boiler which has one hole in a bathtub.
*, $P < 0.01$. **, $P < 0.1$.

the use of a bathroom dryer or a ventilating fan to decrease the recovery rate of MAC ($P = 0.08$, Mann-Whitney's U test). Our results showed that the reservation of bathtub water and/or the continuance of high humidity in the bathroom appear to be conducive to MAC colonization.

DISCUSSION

The characteristics of pulmonary MAC disease, frequent recurrence and multiple infections, suggest that polyclonal MAC colonization is likely to occur in the home or hospital environment surrounding patients. Here, we demonstrated that polyclonal MAC organisms colonize predominantly inside the showerhead and the bathtub inlet of patients' bathrooms. In our previous study, MAC isolates were recovered from residential bathrooms but not from other sites within the residence (17). This uneven distribution and polyclonal colonization of MAC in the residential bathrooms suggested that MAC concentrates and colonizes in the bathroom preferentially. Furthermore, we found that MAC organisms colonized in the bathrooms for a long period of at least 3 months. These findings were in accord with a previous report that nontuberculous mycobacteria (including MAC) formed persistent colonies in a drinking water system (20). Thus MAC may also persistently colonize in bathtub inlets and the inside of the showerhead, where biofilm can be formed.

For 7 cases (47%, 7/15), the genotypes of the environmental isolates showed PFGE patterns related to their respective clinical isolates. Such a high rate of related polymorphism suggests that the bathroom is one of source of infection, although there is still a possibility that MAC bacilli might be transmitted from patients to their bathrooms. Therefore, the source of primary infection with MAC is a controversial issue. However, the fact that patients' bathrooms colonize MAC supports the idea that patients were reinfected by inhaling the MAC organisms each time they bathed. When patients repeatedly inhale pathogens, the efficacy of chemotherapy is reduced, and reinfection may be caused by the same pathogen or a genetically different strain. In fact, the cure rate with macrolide-based regimens is still low, and MAC infection frequently recurs after the sputum culture is converted to negative upon successful completion of therapy (2,3,9). Most recurrences of MAC disease after discontinuation of therapy are interpreted as reinfections with new MAC strains rather than relapse of the initial MAC strains (3,7,8). In the present study, we also demonstrated that the genotypes of reinfected strains were related to those of isolates from their respective bathrooms. This fact supports a risk of reinfection in patients. Furthermore, polyclonal infection may be involved in transferring organisms from a polyclonal environmental colonization in the bathrooms to patients. A recent report also provided evidence that showers may serve as a source of pulmonary infection caused by waterborne *M. avium* (21). The results of our questionnaire survey suggest that, in order to prevent the transference of MAC from bathroom to patient, it is important to keep the bathroom free from MAC colonization by desiccating. Indeed, Archuleta et al. (22) reported that desiccated *M. avium* loses its viability at a constant rate. It is difficult to prove that the bathroom is the source of primary infection for pulmonary MAC disease. In part, this is because pulmonary MAC disease is often asymptomatic during the early stage of infection and progresses slowly, so that many patients are uncertain of the number of months or years that have passed since the initial infection. If MAC bacilli in the bathroom are transferred to a susceptible host, they might be capable of moving between the bathroom and host during the asymptomatic time periods. Therefore, a prospective cohort study would be required to clarify that the bathroom is a source of infection.

In conclusion, we found that polyclonal MAC organisms were distributed throughout the bathrooms of our patients, but predominantly colonized in the bathtub inlets. Nearly half of the 15 bathrooms that harbored MAC strains (47%, 7/15) had strains with a genetically close relationship to their respective clinical isolates. Thus, it is considered that there is a risk of infection in bathrooms colonized by MAC.

ACKNOWLEDGMENTS

We are grateful to all participants who donated samples and the hospital nurses who took part in our study.

This research was supported by grants-in-aid from the Institute for Fermentation, Osaka (IFO), the Ministry of Education, Culture, Sports, Science and Technology, the Ministry of Health, Labour and Welfare (Research on Emerging and Re-emerging Infectious Diseases, Health Sciences Research Grants), the Japan Health Sciences Foundation, and the United States-Japan Cooperative Medical Science Program against Tuberculosis and Leprosy.

REFERENCES

1. Falkinham, J.O., 3rd (1996): Epidemiology of infection by nontuberculous mycobacteria. Clin. Microbiol. Rev., 9, 177-215.
2. Field, S.K., Fisher, D. and Cowie, R.L. (2004): *Mycobacterium avium* complex pulmonary disease in patients without HIV infection. Chest, 126, 566-581.
3. Griffith, D.E., Aksamit, T., Brown-Elliott, B.A., et al. (2007): An official ATS/IDSA statement: diagnosis, treatment, and prevention of nontuberculous mycobacterial diseases. Am. J. Respir. Crit. Care Med., 175, 367-416.
4. Sakatani. M. (2005): The non-tuberculous mycobacteriosis. Kekkaku, 80, 25-30 (in Japanese).
5. Marras, T.K. and Daley, C.L. (2002): Epidemiology of human pulmonary infection with nontuberculous mycobacteria. Clin. Chest Med., 23, 553-567.
6. Songer, J.G., Bicknell, E.J. and Thoen, C.O. (1980): Epidemiological investigation of swine tuberculosis in Arizona. Can. J. Comp. Med., 44, 115-120.
7. Wallace, R.J., Jr., Zhang, Y., Brown, B.A., et al. (1998): Polyclonal *Mycobacterium avium* complex infections in patients with nodular bronchiectasis. Am. J. Respir. Crit. Care Med., 158, 1235-1244.
8. Wallace, R.J., Jr., Zhang, Y., Brown-Elliott, B.A., et al. (2002): Repeat positive cultures in *Mycobacterium intracellulare* lung disease after macrolide therapy represent new infections in patients with nodular bronchiectasis. J. Infect. Dis., 186, 266-273.
9. Kobashi, Y. and Matsushima, T. (2003): The effect of combined therapy according to the guidelines for the treatment of *Mycobacterium avium* complex pulmonary disease. Intern. Med., 42, 670-675.
10. Subcommittee of the Joint Tuberculosis Committee of the British Thoracic Society (2000): Management of opportunist mycobacterial infections: Joint Tuberculosis Committee Guidelines 1999. Thorax, 55, 210-218.
11. Aronson, T., Holtzman, A., Glover, N., et al. (1999): Comparison of large restriction fragments of *Mycobacterium avium* isolates recovered from AIDS and non-AIDS patients with those of isolates from potable water. J. Clin. Microbiol., 37, 1008-1012.
12. Covert, T.C., Rodgers, M.R., Reyes, A.L., et al. (1999): Occurrence of nontuberculous mycobacteria in environmental samples. Appl. Environ. Microbiol., 65, 2492-2496.
13. Falkinham, J.O., 3rd, Norton, C.D. and LeChevallier, M.W. (2001): Factors influencing numbers of *Mycobacterium avium*, *Mycobacterium intracellulare*, and other mycobacteria in drinking water distribution systems. Appl. Environ. Microbiol., 67, 1225-1231.
14. Peters, M., Muller, C., Rusch-Gerdes, S., et al. (1995): Isolation of atypical mycobacteria from tap water in hospitals and homes: is this a possible source of disseminated MAC infection in AIDS patients? J. Infect., 31, 39-44.
15. Arbeit, R.D., Slutsky, A., Barber, T.W., et al. (1993): Genetic diversity among strains of *Mycobacterium avium* causing monoclonal and polyclonal bacteremia in patients with AIDS. J. Infect. Dis., 167, 1384-1390.
16. von Reyn. C.F., Maslow, J.N., Barber, T.W., et al. (1994): Persistent colonisation of potable water as a source of *Mycobacterium avium* infection in AIDS. Lancet, 343, 1137-1141.
17. Nishiuchi, Y., Maekura, R., Kitada, S., et al. (2007): The recovery of *Mycobacterium avium-intracellulare* complex (MAC) from the residential bathrooms of patients with pulmonary MAC. Clin. Infect. Dis., 45, 347-351.
18. Ad Hoc Committee of the Scientific Assembly on Microbiology, Tuberculosis, and Pulmonary Infections (1997): Diagnosis and treatment of disease caused by nontuberculous mycobacteria. This official statement of the American Thoracic Society was approved by the Board of Directors, March 1997. Medical Section of the American Lung Association. Am. J. Respir. Crit. Care Med., 156, S1-25.
19. Chen, Z.H., Butler, W.R., Baumstark, B.R., et al. (1996): Identification and differentiation of *Mycobacterium avium* and *M. intracellulare* by PCR. J. Clin. Microbiol., 34, 1267-1269.
20. Hilborn, E.D., Covert, T.C., Yakrus, M.A., et al. (2006): Persistence of nontuberculous mycobacteria in a drinking water system after addition of filtration treatment. Appl. Environ. Microbiol., 72, 5864-5869.
21. Falkinham, J.O., III, Iseman, M.D., Haas, P., et al. (2008): *Mycobacterium avium* in a shower linked to pulmonary disease. J. Water Health, 6, 209-213.
22. Archuleta, R.J., Mullens, P. and Primm, T.P. (2002): The relationship of temperature to desiccation and starvation tolerance of the *Mycobacterium avium* complex. Arch. Microbiol., 178, 311-314.

Cancer Cell International

CANCER CELL INTERNATIONAL

BioMed Central

Primary research

Open Access

Growth inhibition of HeLa cell by internalization of *Mycobacterium bovis* Bacillus Calmette-Guérin (BCG) Tokyo

Akira Kitamura*[1], Sohkichi Mastumoto[2] and Izumi Asahina[1]

Address: [1]Division of Oral and Maxillofacial Surgical Reconstruction and Functional Restoration, Department of Developmental and Reconstructive Medicine, Graduate School of Biomedical Sciences, Nagasaki University, Sakamoto, Nagasaki 852-8588, Japan and [2]Department of Host Defense, Osaka City University. Graduate School of Medicine, Asahi-machi, Abeno-ku, Osaka 545-8585, Japan

Email: Akira Kitamura* - a-kit@nagasaki-u.ac.jp; Sohkichi Mastumoto - sohkichi@med.osaka-cu.ac.jp; Izumi Asahina - asahina@nagasaki-u.ac.jp

* Corresponding author

Published: 2 December 2009

Cancer Cell International 2009, **9**:30 doi:10.1186/1475-2867-9-30

Received: 19 August 2009
Accepted: 2 December 2009

This article is available from: http://www.cancerci.com/content/9/1/30

Abstract

Background: Intravesical BCG immunotherapy is effective for preventing recurrence and progression in none muscle-invasive bladder cancer but the dosing schedule and duration of treatment remain empirical. The mechanisms by which intravesical BCG treatment mediates antitumor activity are currently poorly understood.

Results: HeLa cell infected with *Mycobacterium bovis* Bacillus Calmette-Guérin(BCG) Tokyo which were different multiplicity of infection(MOI). Proliferation of HeLa cell reduced in a dose-dependent manner by live BCG. The cytoplasm of the HeLa cell showed variety lysosomal stages by internalized and interacted BCG.

Conclusion: Proliferated Live BCG secreted the protein and depressed the growth of tumor. The possibility for clinical introduction of BCG therapy for carcinoma reported with review of literature.

Background

Intravesical BCG treatment has been demonstrated to be an effective therapy for superficial transitional cell carcinoma of the bladder though the mechanism of antitumor effect still remained unclear. We studied to whether the BCG depressed the growth of malignant tumor cell or not. The proliferation of HeLa cells were inhibited by dose dependent manner infected by live BCG. HeLa cell infected by live and dead *Mycobacterium bovis* Bacillus Calmette-Guérin(BCG) Tokyo revealed variety stage of lysosome and BCG in the cytoplasm of HeLa cell. The internalization of live BCG into the HeLa cells did not blocked by heparin and cytochalasin B. The internalized live BCG secreted the secreted-protein and depressed the growth of tumor cell. Live BCG inhibited the growth of tumor cell by internalized and then the secreted protein in cytoplasm of HeLa cells suggested the possibility of new cancer therapy made of BCG combined with the drug delivery system(DDS).

Results

The growth of HeLa cell was inhibited by dose dependent manner cultured by live *Mycobacterium bovis* Bacillus Calmette-Guérin(BCG) Tokyo (Figure 1). The proliferation of HeLa cell was not inhibited when the MOI was 1. Live BCG indicated more depressed the growth of HeLa cell

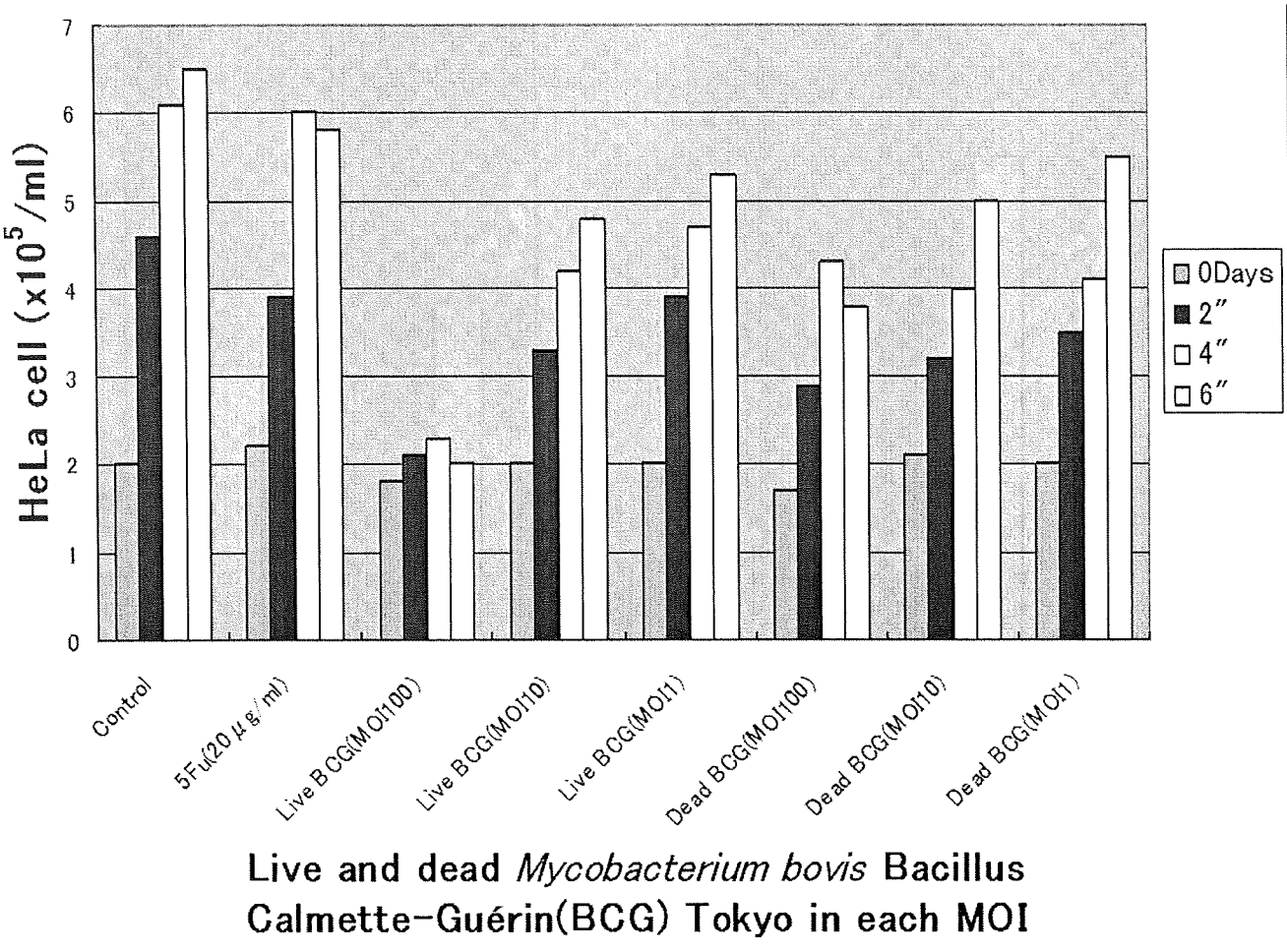

Figure 1
Growth of HeLa cells were depressed by live and dead *Mycobacterium bovis* Bacillus Calmette-Guérin(BCG) Tokyo in each multiplicity of infection(MOI). The growth of HeLa cells were inhibited in dose dependent manner cultured by live BCG. The proliferation of HeLa cell was not inhibited when the MOI was 1.

than the each membrane(0.04 μg/ml, dry weight) or cytoplasm(0.02 μg/ml, dry weight) fraction of the BCG [1] whose dosage were equivalent of MOI 100 (Figure 2).

Two days after cultured with live BCG (MOI 100), HeLa cell showed vacuole and BCG in the cytoplasm (Figure 3A). Even one hour after cultured with live BCG, the cytoplasm of HeLa cell also revealed lysosome, residual body and BCG (Figure 4A). There were several kinds of lysosome which indicated phagocytosis caused from internalized BCG (Figure 4A, C). The myelin-like multilamellar structure was also recognized in the cytoplasm of HeLa cell by dead BCG one day after incubated [2] (Figure 4C). Internalized live or dead (Figure 4A, C) BCG induced the lysosomal activity of the HeLa cell. Four days after the infected HeLa cell by live BCG showed the necrosis in which the BCG kept its shape (Figure 4E). The internalization of live BCG into the HeLa cells was found in their cytoplasm with cytochalasin B [3] (100 μg/ml, Figure 3E) or heparin [4] (0.001 U/ml.Figure 3F) was added into each well before co-culture with HeLa cell respectively. Immunoelectron microscope checked using polyclonal antibodies of the MPB70 (secreted protein, α-antigen) [5-7] and revealed the protein A gold reacted around the cell wall of live BCG. (Figure 3B, D)

Discussion

Intravesical Bacillus Calmette-Guérin(BCG) therapy has been effective in delaying or preventing recurrence and progression for transitional cell carcinoma of bladder although its outcome is still unpredictable [8]. The report suggested that BCG interacted with tumor cells or internalized into them, and yet the role of cellular attachment has been un-established. Therefore we initiate studied

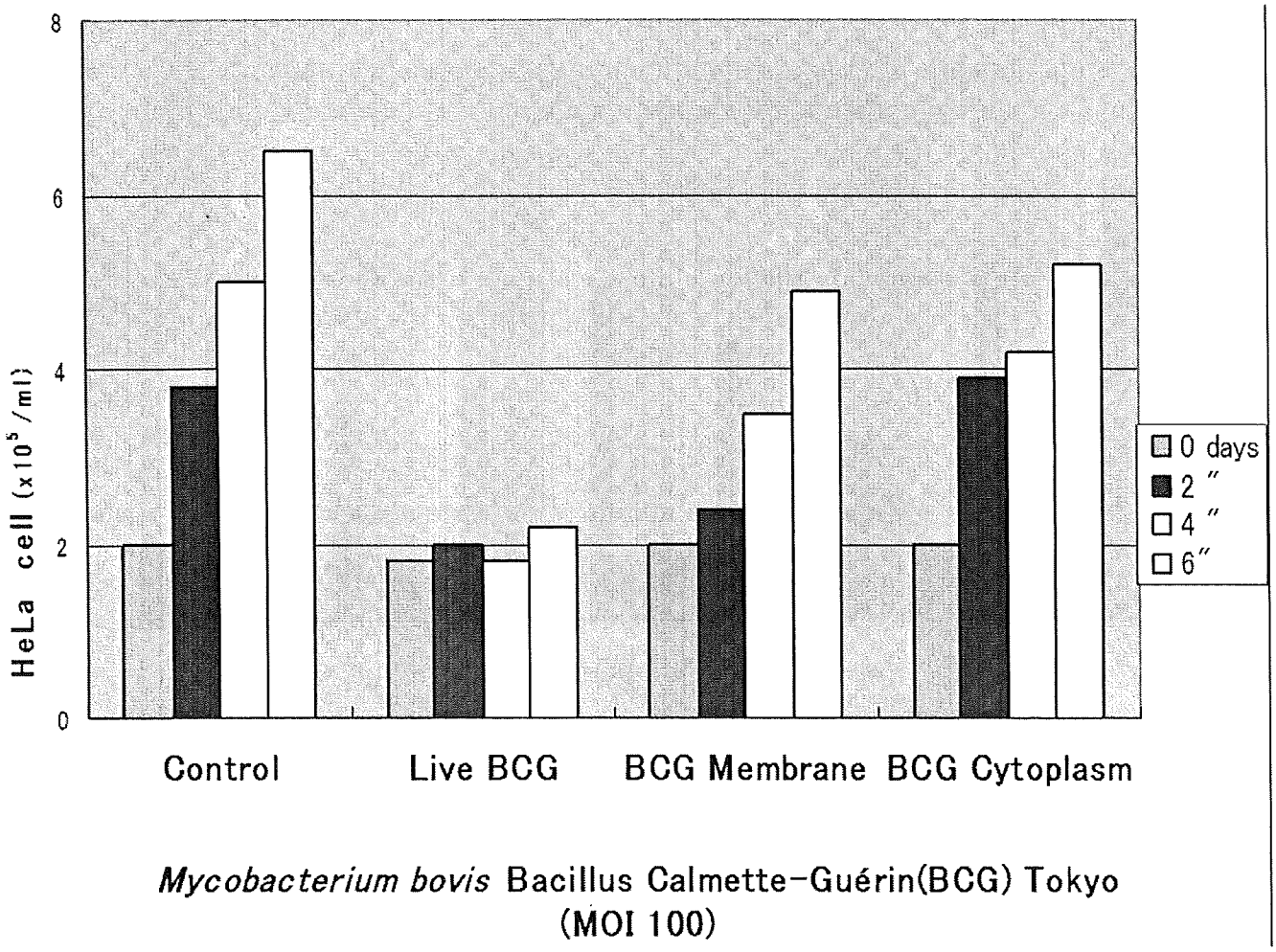

Figure 2
Growth depression of HeLa cell by different BCG component(MOI 100). Live BCG depressed the tumor growth than that of the membrane(0.04 μg/ml, DW) and cytoplasm(0.02 μg/ml, DW) fraction each dosage were equivalent of MOI 100.

using the TEM to better define for the interaction of HeLa cells with BCG and leading to the hypothesis that live BCG induced anti-tumor activity in the tumor cells. The growth inhibition of the HeLa cell was more distinct by live BCG to compare dead BCG, the cytoplasm or membrane fraction of BCG [1]. Those indicated live BCG invaded and proliferated in the tumor cells. Since BCG infection inhibits the proliferation and differentiation of HeLa cells, question arises as to the mechanism whether inducing the bacteriological function from inside or outside. Several bacterial components have already been reported the affected proliferation by infection [9]. The possibility remains that poor nutrition of the cells caused by intracellular proliferation of BCG as well as the BCG stimulus on the cell surface receptor may also be involved in the suppression of cellular proliferation and differentiation [2].

Infection and growth of live BCG in the host cell and released BCG-related cytokine were estimated as the reasons for the depression of the tumor cells. MPB70 [7] (α antigen) known to be an immunogenic mycobacterial protein secreted in large amounts from culture filtrated of *Mycobacterium bovis* Bacillus Calmette-Guérin(BCG) Tokyo. This protein is thought to be crucial for binding phagocytic cell having fibronectin receptors and this function might be a direct effect of BCG immunotherapy[10,11]. BCG is thought to bind to the bladder wall via interaction between the bacterial antigen complex and fibronectin [12]. Similar observations with fibronectin attachment protein(FAP) demonstrated a Type I response inducing IL12 and IFNγ production in normal human peripheral blood lymphocytes. These data suggest that a Type I response is required for antitumor activity by BCG [13].

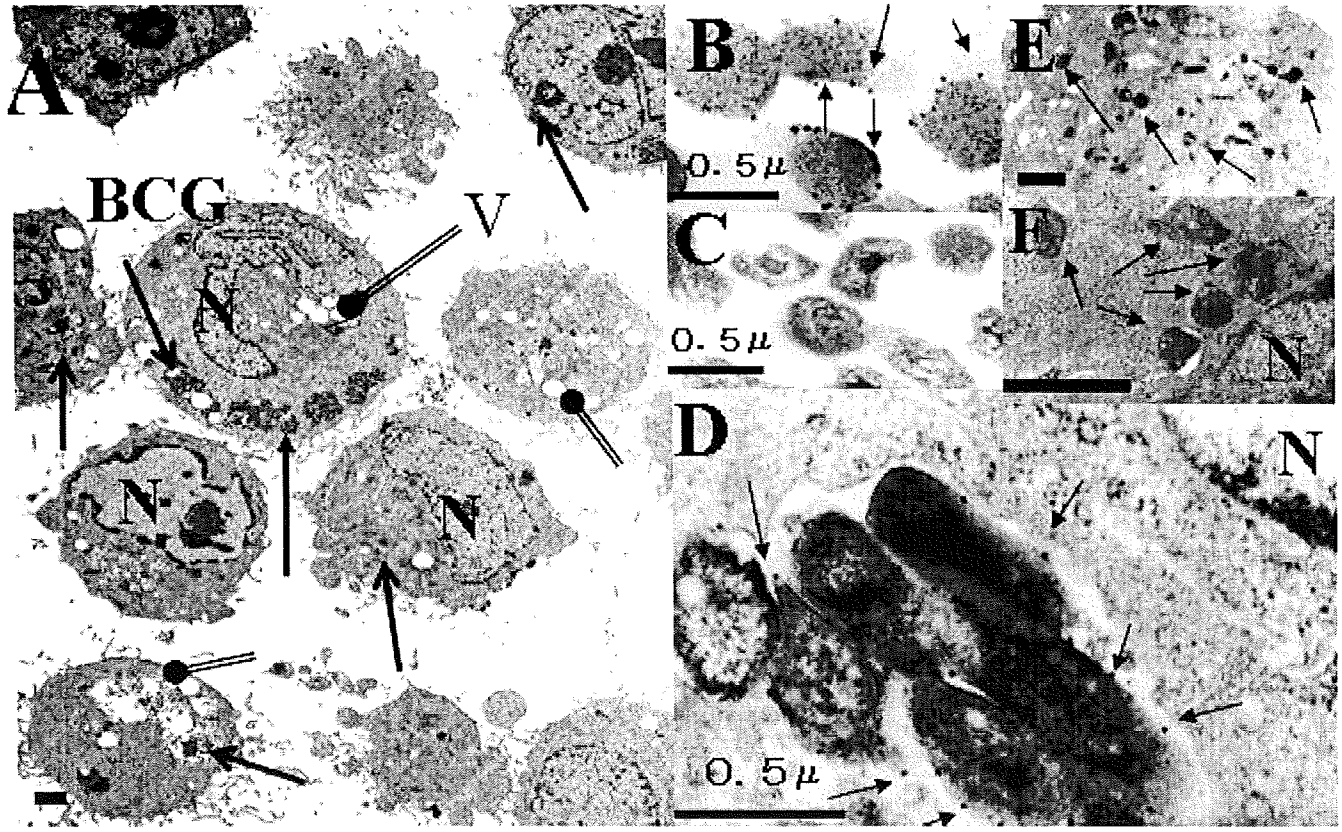

Figure 3

A; HeLa cell and live BCG were co-cultured after 2 days. There were vacuole(V) and BCG(↑) in the cytoplasm of HeLa cell. B, D; Protein A gold(↑) attached on the cell wall of BCG in the HeLa cell co-cultured with live BCG after two days by immunoelectron microscope (anti MPB70 polyclonal antibody). C; Dead BCG did not reacted at the cell wall. Cytochalasin B (E, 100 μg/ml) or Heparin (F, 0.001 U/ml) was added in each culture well of HeLa cell before infection by live BCG also showed the internalized BCG(↑) after 24 hours. N; Nucleus

Antitumor effects of BCG against superficial urinary bladder cancer were known to be strong when BCG is directly infused into the bladder, but its immunological mechanisms are poorly understood [14]. The internalization was inhibited by cytochalasin B(200 μg/ml)[3]; conditions known to inhibit phagocytosis [15]. Heparin (1.25 U/Kg) also induced the aggregation of the local expression of fibronectin and sequentially lessen FN-mediated BCG attachment to bladder wall [4]. But cell membrane-expressed fibronectin did not seem to be crucially involved in the internalization of BCG by transitional bladder cancer. A correlation between cellular fibronectin expression and the ability of transitional cell carcinoma to internalize BCG may be considered as a fortuitous coincidence [16]. Our data showed the internalization of live BCG into the HeLa cells were not blocked by heparin or cytochalasin B. These phenomena suggested another possible reaction between the membrane of the HeLa cell and BCG. Further experiments will be necessary to clarify the biological relevant related between the internalization and phagocytosis or autophagy which is associated with the role of mycobacterial infection and intracellular killing of the cell [17]. Autophagy, the process in which cellular organelles are targeted for degradation in lysosome, represents another potential tumor resistance mechanism and further adding to the complexity of cell death pathways when tumor cells are exposed to various agents [18,19]. IFN-γ induction of autophagy has not been previously reported in immune or phagocyte cells but has been observed in HeLa cells [2,20]. We reported that mycobacterial infection induces the Th1-type immune response lead on the immunological environment rich in IFN-α, which is a suppressive mediator of the Th2-type immune reaction [21]. Th1-stimulating cytokines played an important role in BCG-induced macrophage cytotoxicity and that combination of BCG with selected Th1-stimulating cytokines, either supplemented or expressed by BCG, may enhance the effect of BCG in the treatment of bladder cancer patients [22]. Early stages of BCG infection into osteoblastic-like cell (MC3T3-E1) secreted IL-6 and then

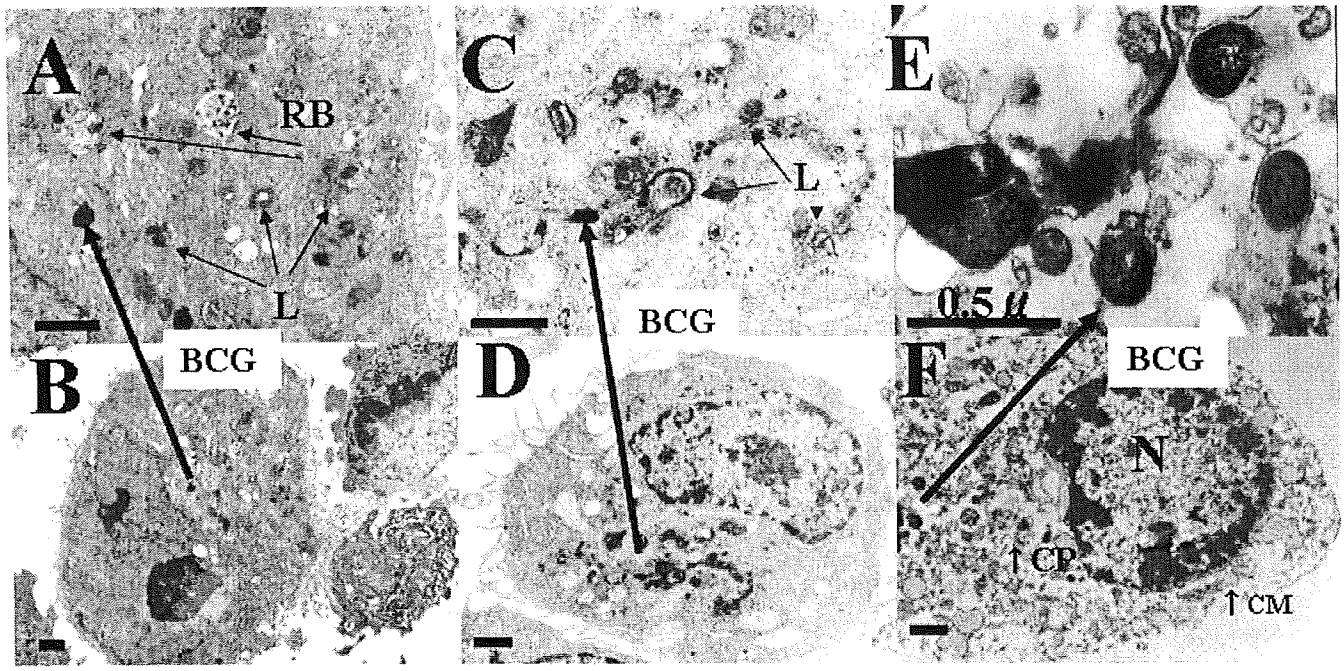

Figure 4
A, B; HeLa cells were infected with live BCG after 1 hour and showed BCG(↑), residual body(RB) and lysosome(L) in the cytoplasm. Different stages of the lysosomal activity were induced by internalized BCG. C, D; HeLa cells were co-cultured with dead BCG(↑) which were also internalized after 1 hour and showed the lysosome and vacuole. E, F; HeLa cells co-cultured with live BCG after four days. HeLa cell showed lack of cell membrane(↑CM), lost of cytoplasm(↑CP), nuclear degeneration(N) and BCG(↑). The shape of BCG was keeping in the HeLa cell.

depressed the proliferation of host [23]. The findings that live BCG infected and internalized in the HeLa cells as shown here, lysosomal activity is an important connection between immune mediator and associated intracellular depression of the host cells. These data suggested that live BCG invaded and proliferated in the cell then released the BCG-related protein have direct effect to inhibit the growth of the host.

The novel method such as using target would allow further improve the bacteria to satisfy a variety of requirements for clinical use. These therapies elicit active immune response against the tumor so that they kill off primary as well as metastases [24]. Successful cancer therapy required close contact between BCG and tumor cells, a host capable of developing and expressing delayed hypersensitivity type reactions to mycobacterial antigens, limited tumor size and an adequate number of viable BCG [25]. It is also necessary to establish the effective drug delivery system(DDS) to be internalized into malignant cell in vivo treatment [26]. The difference between the live and dead BCG which internalized in the cytoplasm of HeLa cell is the existence of secreted protein or not. BCG interacted with tumor cells and were internalized into them suggested future development of anti-tumor agents made from bacterial cell wall [27]or secreted protein [28].

Conclusion

Live BCG depressed the growth of the HeLa cell by dose dependent manner.

Live BCG internalized and secreted protein in the host cell suggested the depression of tumor cell.

Methods

HeLa cell

HeLa cell (1×10^5 cells/ml) were maintained in minimal essential medium (MEM, Gibco BRL, Tokyo Japan) supplemented with 10% fetal bovine serum and 100,000 U/1 penicillin at 37°C in humidified atmosphere with 5% CO_2. The cultured medium was replaced every 3 days. Cells were rinsed 2 times with phosphates-buffered saline (PBS; 137 mM NaCl, 2.7 mM KCl, 8.1 mM NaH_2PO_4) before addition of fresh medium.

Bacillus Calmette-Guérin(BCG) [7,1,29]

Mycobacterium bovis Bacillus Calmette-Guérin(BCG) Tokyo was cultured in Middle brock 7H9 broth (Difco Laboratories, Detroit, MI, USA) supplemented with 10% Albumin-dextrose-catalase(ADC; Difco laboratories) enrichment and 0.1% Tween 80. The cells(approximate 8×10^{10} cells/ml) were harvested with shaking at 37°C until 0.8 of an optical density(OD) at 590 nm. It was centri-

fuged and the pelletized cells re-suspended with MEM were divided and used for experiments. Dead BCG dosage (1×10^7 cells/ml) as MOI 100 was prepared and treated by an autoclave (121°C, 10 min).

Fraction of BCG membrane and cytoplasm [1]

BCG(Tokyo) was sedimented (3,000 × g, 10 min, 4°C), suspended in TMNSH buffer, and lysed by sonication in a Bioruptor UCD-200T sonicator (Toso, Tokyo, Japan). The cell lysate was centrifuged at 10,000 × g for 10 min at 4°C twice. The supernatant was then centrifuged at 30,000 × g for 30 min at 4°C. The pellet was used as the membrane fraction.

The supernatant solution was centrifuged under the same conditions, and the supernatant thus obtained was then centrifuged at 105,000 × g for two hours at 4°C. The pellet was used as the cytoplasm fraction.

The pellets obtained in each step were suspended in TMNSH buffer. Freeze drying membrane and cytoplasm fraction were prepared 0.04 μg/ml and 0.02 μg/ml respectively for the experiment as MOI 100 and keeping at the department of oral bacteriology Nagasaki University. BCG also had been cultured in the same department.

Polyclonal antibody [7]of MPB70 (secreted protein, antigen) [5,6,10]

Purified MPB70 was provided by Dr. Nagai. BALB/c mice at 7-10 weeks of age were immunized intravenously with MPB 70 (10 μg diluted 200 ul of PBS) which was served as the most abundant protein in the culture filtrate from BCG(Tokyo). After 30 days, same amount of MPB 70 was injected intraperitoneally to boost the immune response. After 1 week later, sera were collected from the eye vein of immunized mice and pooled at -80°C until use. Animal had been keeping at animal center of Nagasaki Univ.

HeLa and BCG cells co-culture

Two millimeter of HeLa cells (1×10^5/ml) were inoculated in 24-well plates and cultured for 1 days. Then BCG at various doses and type were added to the wells. After 72 hours fresh MEM exchanged one ml.

Different BCG dosage even, ten and hundred times of multiplicity of infection (MOI) BCG were prepared and cultured with HeLa cell.

Growth inhibition of HeLa cell checked by its fraction of membrane (0.04 μg/ml, Dry weight) and cytoplasm (0.02 μg/ml, Dry weight) were also prepared as equivalent dosage of MOI 100 and added in the medium of HeLa cells.

Internalization of the BCG checked using each cytochalasin B (100 μg/ml, Wako pure C.I. Japan) or heparin sodium (0.001 U/ml, OSTUKA Pharm. Japan) was added into the well before co-cultured with HeLa cell respectively.

Cell count

Every other day during the incubation period with the HeLa and BCG, MEM changed to the usual saline solution and treated 2% tripsin treated for 5 minutes. HeLa cells were mounted on the erythrocytometer after 0.3% trypan-blue stain. The number of cells expressed as the mean for three times.

Transmission electron microscope (TEM) [28]

The HeLa cell washed in the normal saline solution and centrifuged. The cells were fixed in solution of 2% glutaraldehyde in 0.1 M phosphate buffer solution, pH 7.3 for 2 hours and 1% osmium tetraoxide for 2 hours. After two times washed PBS and water the cells were dehydrated with increasing concentrations of ethanol; and gradually infiltrated with Epon 812. Before inspection by TEM the trimmed bloc of epon was orientated and stained with toluidine blue for light microscopy orientation. The ultrathin section with silver to gold interference color were picked up in a nickel grid and stained with uranyl acetate and lead nitrate in the usual manner.

For Immuno-TEM HeLa cell fixed 1% paraformaldehyde at 4°C for one hour. Then dehydrated in ethanol and embedded by LR white(Okenshoji, Japan) for 2 days at -20°C. The same interference color picked up on the collodion coated mesh (Nissinn EM, Japan) specimens were reacted with 2% hydrogen peroxide for 30 minutes twice and blocked bovine serum for 30 minutes. They were reacted with hundred times diluted anti-sera (polyclonal Aanti-MPB70) for 12 hours at 8°C and protein A gold (15 nm, FUNAKOSI, Japan) for three hours at room temperature in moisture chamber and then double stained for 5 minutes each. The specimens were examined in a H800 electron microscope (Hitachi, Japan) operating at 75 kV.

Competing interests

The authors declare that they have no competing interests.

Authors' contributions

AK counted the HeLa cells, carried out the morphologic study of TEM and immuno-TEM, drafted the manuscript and designed this experiment. SM cultured the BCG, prepared MPB70 and BCG fraction of membrane and cytoplasm and made the polyclonal antibody of MPB70 (secreted protein, α-antigen). IA carried out the co-culture of BCG and HeLa cell. All authors read and approved the final manuscript.

References

1. Ohara N, Naito M, Miyazaki C: **HrpA, a new ribosome-associated protein which appears in heat-stressed *Mycobacterium bovis* Bacillus Calmette-Guérin.** *J Bacteriol* 1997, **179**:6495-6498.